INVESTIGATION OF ACOUSTIC FIELD NON-LINEARITIES BY SUSPENSION OF PARTICLES IN A CYLINDRICAL RESONATING CAVITY

by

NEIL L. FLEISHON

Submitted in Partial Fulfillment
of the Requirements for the
Degree of Bachelor of Science
at the
Massachusetts Institute of Technology
June 1973

Signature of the Author . . . Signature redacted .
Department of Physics, May 10, 1973

Certified by . . . . . Signature redacted
Professor K.U. Ingard, Thesis Supervisor

Accepted by . . . . . Signature redacted .
Chairman, Departmental Committee on Theses

INVESTIGATION OF ACOUSTIC FIELD NON-LINEARITIES BY SUSPENSION OF PARTICLES IN A CYLINDRICAL RESONATING CAVITY

I. Abstract

Non-linear behavior of high amplitude acoustic waves is investigated by observation of non-zero time average forces predicted by a second order perturbation theory analysis. A theoretical description is given of the force on a sphere in a cylindrical cavity driven at resonance due to field non-linearities.

These forces are observed in a cylindrical cavity driven at resonance at 155-165 dbs. A qualitive description of these effects is given for particles of millimeter order. Quantitive measurement of non-linear forces is made by suspension of spheroids of diameters of centimeter order. The behavior of the forces with respect to experimental variables is found to be in substantial agreement with prediction within the limits of experimental accuracy.

II. Table of Contents

III. Introduction

Expressions for the acoustic variables, fluid density, fluid velocity, and fluid pressure can be obtained by linearizing the equations governing fluid motion, neglecting the internal energy loss terms. These expressions are valid for low sound pressure levels below 145 db. The accuracy of the first order decreases as the sound level is raised, due to the contribution of second order effects which increase as the square of the pressure amplitude of the first order. In the range between 145 and 160 dbs., the second order effects become non-negligeable but still small compared to the total function. In this region a perturbation approximation is a valid description of the physical situation. As the sound level is raised to above 165 db., the higher orders become so large that it makes no sense to use the perturbation analysis. In this case, the medium is said to be "shocked."

In the first order, the time dependence of the fluid variables is sinuosoidal, giving time averages which equal zero. The second order is, however, non-linear, and will include terms which are products of two first order variables, giving rise to $\sin^2$ and $\cos^2$ terms in the time dependence. In the second order, then, the acoustic variables have a definite non-zero time average value.

In particular, the non-zero time average pressure field gives rise to definite steady state forces. The nature of these forces in a cavity at resonance have been the subject of investigation for some time. Investigation has been carried out by observation of fluid deformation in rectangular geometry,[1,2] by observation of dust particle patterns,[3] etc.

In the present experiment the magnitude of the non-linear forces is measured by balancing it against a constant, known force, that of gravity. This is done by using the non-linear forces to keep a small, light spheroid in suspension in a cylindrical cavity driven at its purely longitudinal resonance modes. The sound pressure level needed to sustain this suspension is measured as a function of varying sphere mass, resonant frequency, and sphere size, and the results compared to theoretical prediction.

IV. Theory

A. General

The fundamental equations governing fluid flow are expressions of mass and momentum conservation and the ideal gas law. In these equations

$\rho(r,t)$ = total fluid density

$v(r,t)$ = total fluid velocity

$p(r,t)$ = total fluid pressure

These equations are partial differential equations, the partial derivative operator indicating that these equations are written in the Eulerian frame of reference, in which the change in a fluid function is measured at a fixed point as the fluid streams past.

1. Equation of Continuity

$$\frac{\partial \rho(r,t)}{\partial t} + \nabla \cdot \left(\rho(r,t)\, v(r,t) \right) = Q \qquad (1)$$

This equation states that the rate of change of material in a region is equal to the net flow of material into that region plus the net rate of creation in the region. Q is the creation term, determined by the placement of material sources and sinks. If there are no sources or sinks, Q is zero and equation (1) becomes

$$\frac{\partial \rho(r,t)}{\partial t} = - \nabla \cdot \left(\rho(r,t)\, v(r,t) \right) \qquad (2)$$

2. Newton's Second Law

$$\rho(r,t) \left[\frac{\partial v(r,t)}{\partial t} + v(r,t) \cdot \nabla v(r,t) \right] = - \nabla p(r,t) \qquad (3)$$

3. The Ideal Gas Law

The thermodynamic variable, the bulk compressibility κ, is defined by the relation

$$\kappa = \frac{1}{\rho} \left(\partial \rho / \partial p \right)_s \qquad (4)$$

The differentiation is for an adiabatic process because the pressure changes are so rapid that there is no heat exchange from one part of the fluid to another.

The equation of state for adiabatic processes in an ideal gas is

$$p = p_0 \left(V_0 / V \right)^{\gamma} = p_0 \left(\rho_0 / \rho \right)^{\gamma} \qquad (5)$$

where p_0, V_0, ρ_0 represent the ambient conditions in the absence of sound

and γ is equal to the ratio of the specific heat of the gas at constant pressure to that at constant volume.

If Δp, the difference between the pressure in a region and the ambient pressure p_0, is small, then $\Delta\rho$, the difference in density from ambient conditions, is given by equation (4) as

$$\Delta\rho = \gamma\kappa\rho_0\Delta p \tag{6}$$

Equations (1), (3), and (6) constitute three equations in three unknowns which, in principle, may be solved exactly. Approximate solutions may be obtained by writing the acoustic variables as:

$$\rho = \rho_0 + \lambda\rho_1 + \lambda^2\rho_2 \ldots\ldots$$
$$\vec{v} = \vec{v}_0 + \lambda\vec{v}_1 + \lambda^2\vec{v}_2 \ldots\ldots$$
$$p = p_0 + \lambda p_1 + \lambda^2 p_2 \ldots\ldots$$

where λ is a "bookkeeping" variable, the zero subscripted variables are the values in the absence of a disturbance, and the integer subscripted variables are the corrections to the ambient values due to a disturbance. In this perturbation analysis $f_n << f_{n-1}$. (f any acoustic variable).

Inserting these solutions into a frame of reference where $v_0=0$, and in a situation where there are no sources or sinks of material gives

$$\frac{\partial}{\partial t}(\rho_0+\lambda\rho_1+\lambda^2\rho_2\ldots) + \nabla\cdot(\rho_0+\lambda\rho_1+\lambda^2\rho_2+\ldots)(\lambda\vec{v}_1+\lambda^2\vec{v}_2\ldots) = 0 \tag{2a}$$

$$(\rho_0+\lambda\rho_1+\lambda^2\rho_2\ldots)\left[\frac{\partial}{\partial t}(\lambda\vec{v}_1+\lambda^2\vec{v}_2\ldots) + (\lambda\vec{v}_1+\lambda^2\vec{v}_2\ldots)\cdot\nabla(\lambda\vec{v}_1+\lambda^2\vec{v}_2\ldots)\right] = -\nabla(p_0+\lambda p_1+\lambda^2 p_2+\ldots) \tag{3a}$$

$$\gamma\kappa\rho_0(\lambda p_1+\lambda^2 p_2\ldots) = (\lambda\rho_1+\lambda^2\rho_2\ldots) \tag{6a}$$

1. First Order Solutions

Equating coefficients of λ in equations (2a), (3a), and (6a):

$$\frac{\partial\rho_1}{\partial t} + \nabla\cdot\rho_0\vec{v}_1 = 0 \tag{2b}$$

$$\rho_0\frac{\partial\vec{v}_1}{\partial t} + \vec{\nabla}p_1 = 0 \tag{3b}$$

$$\rho_1 = \gamma\kappa\rho_0 p_1 \tag{6b}$$

Combining these equations gives the classical linear wave equation for the acoustic variables.

$$\frac{\partial^2 f_1}{\partial t^2} - \frac{1}{\kappa \rho_0} \nabla^2 f_1 = 0 \tag{7}$$

Thus, to the first order, a wave disturbance may be propagated through the fluid medium with the speed $(\kappa \rho_0)^{-1/2}$. From equations (4) and (5)

$$(\kappa \rho_0)^{-1/2} = \left[\left(\frac{\partial \rho}{\partial p}\right)_s\right]^{-1/2} = \left[\gamma \left(\frac{p_0}{\rho_0}\right)\left(\frac{\rho}{\rho_0}\right)^{\gamma-1}\right]^{1/2} \approx (\gamma p \rho_0)^{1/2} \tag{8}$$

if $\rho_1 << \rho_0$. Equation (7) must be solved with respect to the boundary conditions imposed by the specific geometry. This gives the form of the spatial part of the solution. The time dependence of the solution is always sinuosoidal giving:

$$f_1 = \psi(x_1, x_2, x_3)\, e^{i\omega t} \tag{9}$$

The time average of f_1, $\langle f_1 \rangle$, is given by

$$\langle f_1 \rangle = \lim_{t \to \infty} \frac{\int_0^t f_1 \, dt}{t} = \psi \lim_{t \to \infty} \frac{\int_0^t e^{i\omega t} dt}{t} = 0 \tag{10}$$

Thus, none of the first order acoustic variables have non-zero time averages.

2. Second Order Solutions

Equating coefficients of λ^2 in equations (2a), (3a), and (6a) gives:

$$\frac{\partial \rho_2}{\partial t} + \nabla \cdot (\rho_0 v_2 + \rho_1 v_1) = 0 \tag{2c}$$

$$\rho_0 \frac{\partial v_2}{\partial t} + \rho_1 \frac{\partial v_1}{\partial t} + (v_1 \nabla v_1)\rho_0 = -\nabla p_2 \tag{3c}$$

$$\kappa \rho_0 p_2 = \rho_2 \tag{6c}$$

Again, three equations in three unknowns can be solved for the second order correction factor. In general it is not easy to solve these

equations. This difficulty can be circumvented for the present, since the time average of the second order pressure field is the quantity of interest. Operating on equation (3c) with the time average operator gives

$$\rho_0 \langle v_1 \cdot \nabla v_1 \rangle \cong - \vec{\nabla} \langle p_2 \rangle \qquad (3d)$$

The time average pressure calculated in (3d) is an average over terms like $\sin^2$ and $\cos^2$ due to the non-linear $\langle v_1 \cdot \nabla v_1 \rangle$ term. The time average of these terms is non-zero, so that there will be a non-zero pressure field and therefore non-zero forces in the second order.

B. Application to Experiment

Using this theoretical machinery, we try to find the time average force on a sphere in a cylindrical cavity. We are given a sphere of radius a placed in a rigid walled cylinder length L, radius r_0, such that the center of the sphere lies on the central axis of the cylinder. (See Fig. 1)

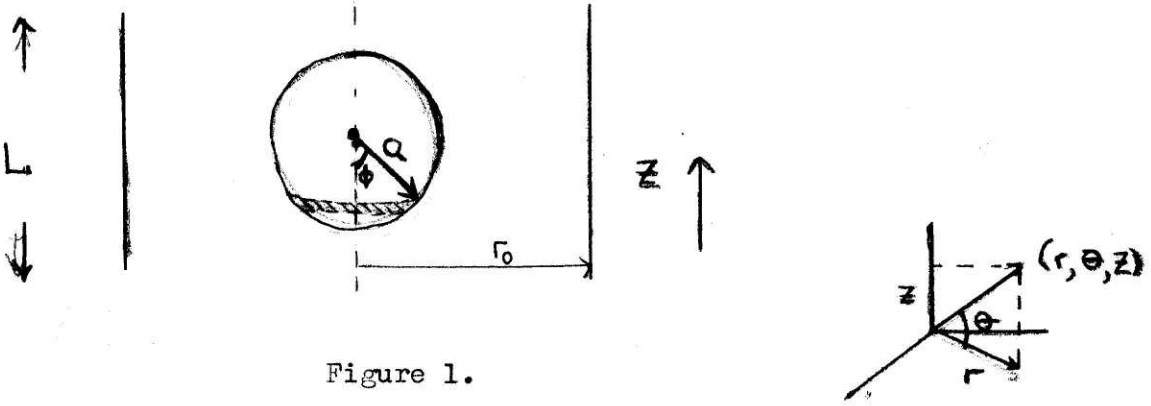

Figure 1.

It is assumed that there is no scattering interaction between the sphere and the pressure field.

The pressure and velocity fields are given to the first order by wave equation (7) with the boundary requirements that the radial velocity be zero at $r=r_0$, that the axial velocity be zero at z=0 and z=L, and that $f(\theta) = f(\theta + 2\pi)$.

The form of the first order pressure field is then given by:

$$p_1 = \sum_{l,m,n} p_{l,m,n} \qquad (11)$$

$$p_{l,m,n} = A_{l,m,n} e^{i\omega_{l,m,n} t} \cos \frac{n\pi z}{L} \left(c_1 e^{im\theta} + c_2 e^{-im\theta} \right) J_m(k_l r)$$

where $A_{l,m,n}$ is the pressure amplitude at $\omega_{l,m,n}$, J_m is a Bessel function of the m-th order. The values of k_l are restricted to those which satisfy the boundary condition on the radial velocity. Further, there is the requirement that

$$k_l^2 + \frac{n^2\pi^2}{L^2} = \frac{\omega_{n,l,m}^2}{c^2} \tag{12}$$

where c is the speed of sound.

Since the system is symmetric about the central axis, $f(r,\theta,z)$ is equal to $f(r,z)$. Thus only $p_{1,0,n}$ terms are included in the sum of equation (11). If the tube is driven at the resonance frequency, $\omega_n = c(\frac{n\pi}{L})$, then $k_l = 0$ and the pressure field is given by

$$p_{0,0,n} = A_n e^{-i\omega_n t} \cos\frac{n\pi z}{L} \tag{13}$$

Thus, at tube resonance, the pressure field is a longitudinal, compressional standing wave, a function of z alone. It is identical to the expression for the (0,0,n) resonance mode of a rectangular cavity.

For the general pressure field in a cylindrical cavity the calculation of the time average second order pressure is not simple. For the resonance pressure field, equation (13), the mathematics is considerably simplified. The solution, obtained by getting v_{ln} from p_{ln} by equation (3b), substituting into equation (3b), and integrating in rectangular coordinates to solve (3b), can be expressed exactly as

$$\langle p_{2n}(z)\rangle = -\frac{A_n^2}{4\rho_0 c^2}\left[1 - \cos\frac{2n\pi z}{L}\right] \tag{14}$$

This expression can be used to calculate the net force on the sphere. Integration of the pressure over the sphere surface is performed by summing of infinitesmal zones at angle Φ to the tube axis. (See Fig. 1) This gives

$$\langle F_z\rangle = -\int_0^\pi \langle p_{2n}(z - a\cos\Phi)\rangle 2\pi a^2 \sin\Phi\cos\Phi\, d\Phi \tag{15}$$

Inserting the expression from equation (14)

$$\langle F_z\rangle = \frac{\pi a^2 A_n^2}{2\rho_0 c^2}\int_0^\pi \cos\frac{2n\pi}{L}(z - a\cos\Phi)\sin\Phi\cos\Phi\, d\Phi \tag{16}$$

This integral can be done exactly by integration by parts. The solution is given by

$$\langle F_z\rangle = \frac{A_n^2 a L}{2\rho_0 c^2 n}\sin\frac{2n\pi z}{L}\left[\frac{L}{2n\pi a}\sin\frac{2n\pi a}{L} - \cos\frac{2n\pi a}{L}\right] \tag{17}$$

V. Design of Experiment

A schematic of the experiment is given in Figure 1.

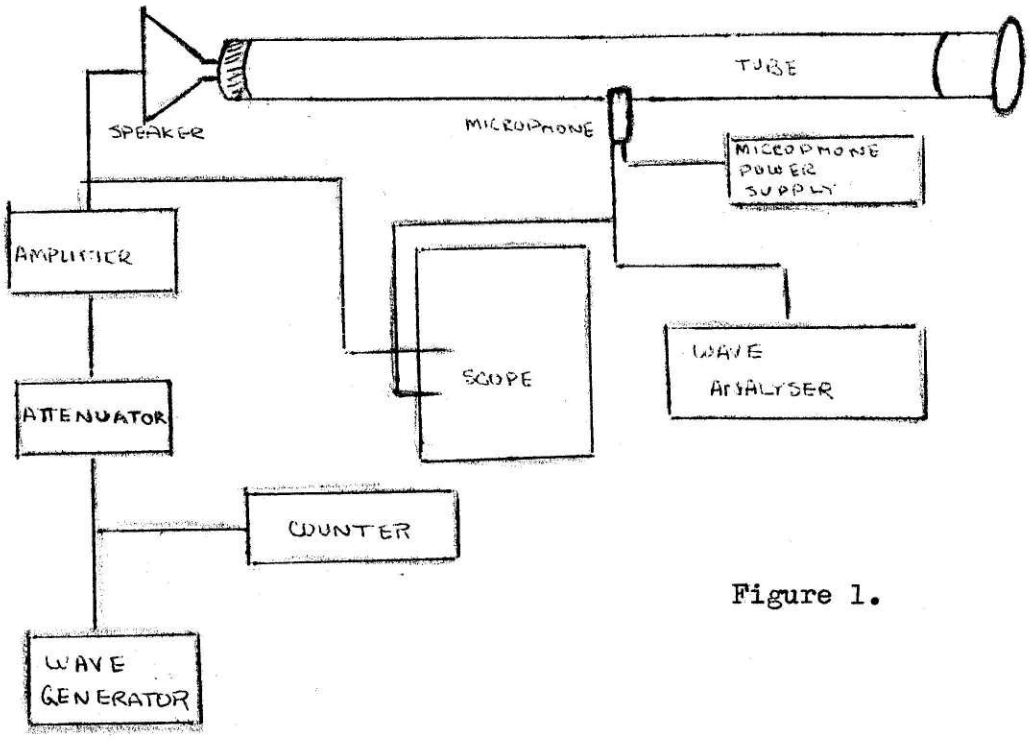

Figure 1.

A. Resonant Cavity

The cavity is a cylindrical plexiglass tube of radius 5.7 cm. with walls of thickness .63 cm. It is stopped at one end by a removable plexiglass cap so that the length of the tube is 175 cm. At the other end, the speaker, an Atlas Sound PD-60T driver with a radius of 1.12 cm. is set into a 2.2 cm. thick aluminum plate which is secured by screws flush against the inner wals of the tube. The speaker is operated at 16 ohms impedence.

B. Signal Production

A 5 volt peak to peak sinuosoidal signal is produced by a Wavetech #110 Function Generator. The frequency of the signal is monitored by a Hewlett Packard #5221B Digital Electronic Counter. The signal is then passed through a scaled variable voltage attenuator which is used as a volume control. Finally, the signal is amplified by a Dynaco Mark III Amplifier by a factor of 28 db. The signal from the amplifier is displayed on a Tektronix #545A Oscilloscope for the purpose of observing the onset of amplifier clipping or

any other signal distortion.

C. Sound Level Detection

A Bruel and Kjaer #4135 quarter inch condenser microphone is inserted into a hole in the tube wall exactly half way along the length of the tube for the purpose of measuring the sound pressure level of standing waves of integer number of wavelengths in the cavity. The condenser microphone is operated with a Bruel and Kjaer #2615 Cathode Follower and #2801 Power Supply. This microphone is characterized by a flat pressure response over the frequency range from 80-10,000 cps., when operated between 64 and 174 db. The harmonic distortion due to the microphone system is less than 1% over this sound pressure range. Variation of sensitivity and response is also insignificant over the ranges of temperature, ambient pressure, and humidity encountered in the experiment. Microphone characteristic graphs may be found in Appendix I.

The microphone output is monitored by the oscilloscope for distortion indicative of impending speaker breakdown. The root mean square voltage of this signal can be measured at any frequency to within 5% by a Hewlett Packard Wave Analyser #302A.

D. Particle Obstacles

All of the particles used in the experiment are made from a low density eccofoam material called Dalon. This substance is widely used as packing material. The Dalon material is in the form of small hemispherical shells of varying sizes in the range of one to two centimeters in radius. The spheroids used are constructed by glueing two hemispheres of the same size together with Duco cement after shaving them down with a penknife in order to make them as light as possible. These spheroids are weighed with a high precision Mettler Type HP 6 balance.

Small particles of millimeter order are made from Dalon by grinding the hemispheres with an ordinary kitchen grater.

VI. Qualitative Observation of Small Particles in the Cavity

A resonant cavity with fine particles in it is usually called a Kundt's tube after the man who first reported his observations of such a system in the 1870's. An excellent account of Kundt's tube characteristics using cork dust is given over a wide range of sound pressure level and frequency by Andrade[4]. The observations described below were all made by Andrade and his descriptive language is used in this account. Photographs of the phenomenae described appear in Appendix II.

We expect the particles, a millimeter or less in size, to more or less behave like the fluid medium. At resonance these particles are observed to clump in regular intervals of one half of the linear wavelength. In addition little ridges appear in regular intervals between these clusters. (Photo 1,2) Particles are observed to fly off these ridges and be pushed in the air toward the nodal clumps. As the sound level is increased, these ridges migrate from the inter-nodal areas (Photo 3,4), a condition called clearance, and gather around the clumps to give a nodal eye structure. (Photo 5)

The particles clump in the minima of the field potential, which occur at the pressure maxima or velocity nodes, occurring at values of z such that $\cos \frac{n\pi z}{L} = 1$. This means that the stable position for a sphere, according to equation (17), should be halfway between two particle clumps. This is observed to be the case. (Photo 6)

The transport mechanism for the particles was first explained by Rayleigh[5] in 1883 by assuming a force of friction between the fluid and the tube walls. He calculated the second order time average velocity at resonance to be

$$\langle u_2 \rangle = \frac{u_1^2}{4c} \sin \frac{2n\pi z}{L} \left[\frac{2r^2}{r_0^2} - 1 \right] \qquad (18)$$

This gives rise to a circulation current in the tube that is sketched in Figure 1.

Figure 1.

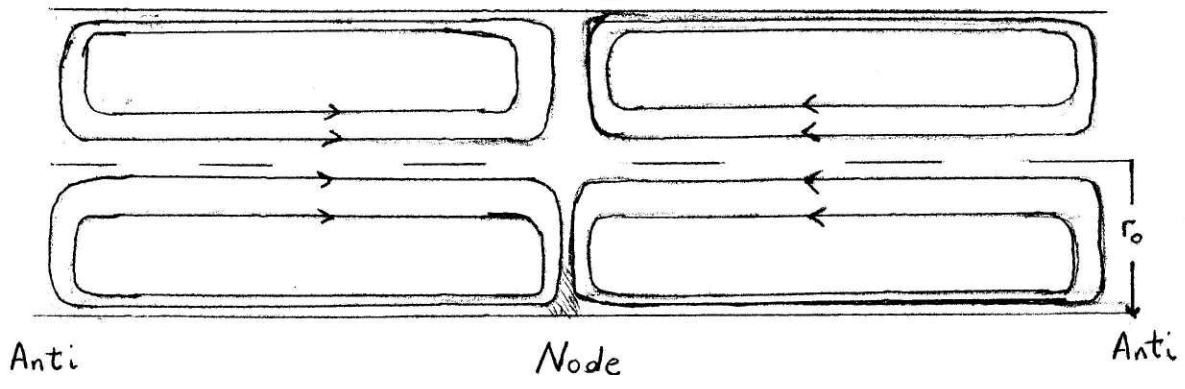

Andrade proposed a mechanism for explaining the wavelet formation and structure due to the buildup of vortex currents due to scattering off particles, causing additional particles to be sucked into the original scattering point. The proposed fluid flow is sketched in Figure 2.

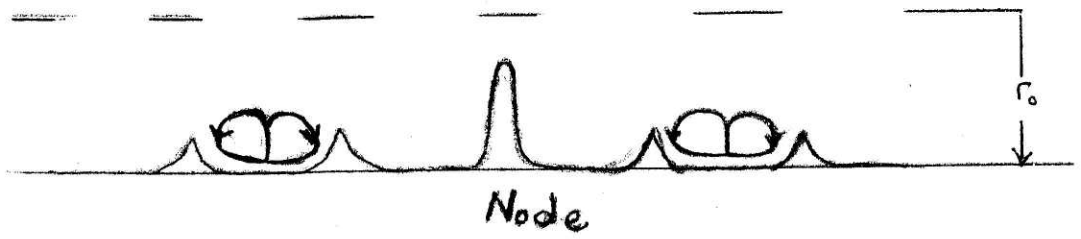

Figure 2

With the tube in the vertical position the particles are suspended in equally spaced layers. (Photo 7) The particles cluster along the tube walls, with some particles seen rising through the center of the tube and being pushed outward in a fountainlike effect like that predicted by the circulation currents of Figure 1. (Photo 8) As the sound level is decreased the larger particles fall. All the particles have fallen by 148-150 dbs (at 764 cps.).

VII. The Experiment

A. Procedure

1. Microphone Calibration

The calibration of the root mean square voltage of the microphone output signal to sound pressure level is achieved by means of a Bruel and Kjaer #4220 Pistonphone. The pistonphone is a small battery driven chamber driven at a known decibel level, 124 db., and frequency, 1000 cps. The microphone is inserted into this chamber by means of coupling adaptors and the R.M.S. output voltage is measured with a Bruel and Kjaer voltmeter.

2. Determination of Resonant Frequencies

The resonant frequencies of the cavity can be determined to within 15 cps. by listening for a loud "shriek" emitted from the tube. This shriek is due to the vibration of the tube walls. By adjusting to the loudest shriek the resonant frequencies can be excellently approximated. As discussed previously, if dust particles are introduced into the cavity, nodal eye structure and clearance occurs at resonance. Determination by these means cuts down the possible frequency error to about 5-8 cps. More exact determination may be made for those resonances where the standing waves consist of integer numbers of wavelengths by using the microphone and observing the voltage output on the oscilloscope for maximim voltage.

A table of the resonant frequencies determined by these means appears in Appendix III A.

3. Determination of Nodes

A node, with regard to this experiment, is used to mean any region where a spheroid may be stably suspended by the field. The positions of these nodes are determined directly and easily at any resonance frequency by suspending a spheroid in the topmost node, turning down the volume to allow the ball to drop, and then quickly increasing the volume again to trap the ball in the next node down. This procedure is repeated to insure that all nodes have been found. Data on the location of nodes in the tube at two resonant frequencies is found in Appendix III B.

4. Microphone Placement

In order to measure the pressure level of the standing waves in the tube, the microphone is placed in a hole drilled halfway along its length. The halfway point is determined by observing the clumping of the small particles at the nodes at resonance. Determination by this means agrees with direct measurement. The microphone is suspended in the cavity by means of an adaptor which comes in contact with it far from the sensitive region. The adaptor and microphone are puttied into place to reduce any possible error due to vibration of the tube walls.

5. Volume Control Calibration

The volume control consists of three knobs, each of ten divisions, corresponding to voltage differences of one-tenth, one, and ten decibels. Thus the voltage going into the speaker is calibrated to a tenth of a decibel. This, however, cannot be used in pressure level calibration due to the fact that the speaker behaves non-linearly in the decibel region used in the experiment (155-165 db.). Calibration to the volume controls is achieved by measuring sound pressure level of the fundamental and the first two harmonics by means of the microphone-wave analyser unit. This measurement is made at intervals corresponding to every one decibel change in incoming voltage. Logarythmic interpolation is used to get the values between the points measured. The calibration is performed at the four resonant frequencies used, also generating distortion graphs which appear in Appendix IV. These curves show the first and second harmonics as a fraction of the fundamental as a function of the decibel level of the fundamental. All sound level data in this experiment is measured at the fundamental.

6. Experimental Procedure

With the tube in a horizontal position the spheroid is placed in the cavity and the top secured. The wave generator is adjusted to one of the four resonance frequencies used and the sound turned up to beyond that expected to be needed to suspend the sphere. The sphere is observed to spin and move in the tube over the space of half a wavelength until it is "caught". It is then held rigidly in one spot.

Since the sphere is not exactly spherical, and the mass not exactly evenly distributed, the orientation of the ball in the tube is important. In general, the spheres are most stable when their largest cross section is presented to the speaker. This is true with the tube both in horizontal and vertical positions. Thus, when the sphere is caught in position, the point closest to the speaker is noted, the ball removed, and the point marked. From then on, all data is taken with the marked point facing the speaker, to insure against error due to change in orientation.

With the spheroid caught, the tube is slowly and gently raised up to a vertical position with the speaker at the bottom. This must be done very carefully because any jolt will cause the sphere to become unstuck from its position. This is especially true when using the lower frequencies because the potential gradient is not as steep as that of the higher frequencies.

In this suspended position the ball rests in contact with the tube walls, from which it cannot be moved. This indicates a non-zero time average radial force outward from the center. In addition, the sphere executes an angular motion, revolving about the central axis of the tube against the walls. This reveals the presence of a non-zero time average component of force in the tangential direction. The sphere's angular speed appears to be a function, not monotonic, of the sound level. Both the angular speed and direction of the motion are very sensitive to the vertical position of the sphere in the tube.

With the sphere suspended the volume is turned down in steps of one division on the one-tenth decibel knob. As the sound pressure approaches the minimum which can support it, the sphere is observed to begin to oscillate about its equilibrium position. This oscillation is probably initiated by the impulse of the transient response to the change in decibel level.

The volume is reduced until the sphere drops. This volume is then recorded and the procedure repeated until a reasonably consistent figure is arrived at. This usually takes about five runs. Data is then taken at the other resonance frequencies used. All data is taken with the sphere in the node closest to the top of the tube.

After these data points are taken the sphere is removed from the cavity and to it is glued a piece of metal cut from a straight pin. The weight of this pin is known from previous weighing. The pin is glued on the spot marked as facing the speaker to insure that the sphere's orientation is

maintained. This effectively heavier sphere is returned to the cavity and new data taken.

The mass is varied by repeating this procedure. The metal pieces are glued alternately on the bottom and top of the ball to try to maintain the center of gravity close to the geometric center, while not introducing any torques tending to change the sphere's orientation.

In this way the minimum supporting sound level as a function of mass for a sphere of fixed radius is measured at several different frequencies. This experiment is performed with four spheroids of different diameter. The data is shown in Appendix III C.

B. Experimental Limitations

1. Limits on Parameter Ranges

Parameter ranges are limited by consideration of various physical aspects of the system.

The upper limit on the frequency used is restricted by the behavior of the speaker above 1000 cps. in the sound level range used. Distortion in the operating region is high and voice coil burnouts are frequent. The lower limit is determined by the ability of the field to consistently trap and hold the sphere. At frequencies lower than those used the potential gradient is not steep enough to keep the ball aloft during the course of the experiment.

The sound level is limited by speaker distortion and breakdown. Breakdown occurs at 165-170 dbs.

The limits on spheroid masses are imposed by consideration of the Dalon material of which the spheres are made. In constructing these spheroids, a compromise must be made between low mass and wall strength. While low mass is desired to increase the range of the experiment, a thin shelled spheroid can be blown apart in the field. This effectively limits the mass lower limit to 125-175 milligrams, depending on the size of the sphere. All the spheres are used until they get blown apart, this determining the upper mass limit. Disintegration of the shell in the field is due not only to the strength of the material alone, but also due to the cement used to glue the pins to the shell, an acetone based glue which interacts with the eccofoam and weakens the wall where it is applied. This weakening is helped along by the vibration of the metal pieces when they are in contact with the vibrating tube walls.

The ranges of sizes and shapes of the spheroids are completely determined by the available building materials. Though the surface of these balls is not smooth, they are, on the average, regular ellipsoids of eccentricity between .2 and .5 with major axes of length between 2 and 3.5 cm.

2. Experimental Difficulties - Sources of Error

Errors due to change in orientation of the spheroid in the tube are considerably decreased by the precautions taken against them which are described above. As a result, the possible error is insignificant compared to other experimental difficulties.

A significant problem is caused by changing the speaker sound volume. The resulting transient response, as discussed briefly above, tends to push the sphere from its equilibrium position. As the volume approaches minimum suspending volume this push from equilibrium may become great enough to knock the sphere from the node. This effect becomes very pronounced at the low frequencies where the gradient is not steep. The resulting error at the low frequency, 383 cps., is on the order of one half of a decibel, and at the next frequency, 574 cps., is about one third of a decibel. The error due to this effect also becomes significant with data on the unweighted sphere due to the fact that there is not as much favoring of a specific orientation of the ball. The transient in this case serves to start the ball spinning. As a result, the sphere falls. Thus the problem of volume change results in measurement of minimum suspending volume higher than the real value, the magnitude of this error being accentuated in low frequency and low mass measurements.

Errors resulting in measurement of minimum suspending volume lower than the real value are due to various frictional problems.

Due to the fact that the suspended eccofoam ball is in contact with the plexiglass wall, there is a tendency for the buildup of static electric charge, resulting in a force of attraction between wall and ball. This effect can be quite pronounced, as the ball has been observed to remain suspended, sticking to the wall, after the driving speaker has been completely turned off. The commercial laundry ingredient, Cling Free, an anti-static fluid spray, is applied to the surface of the sphere before every experimental run as a precaution against this static buildup. The problem with the Cling Free is that it is a greasy substance which also serves to increase the ball-wall friction.

Scratches on the inner wall of the tube also serve to impede the

free motion of the sphere.

There is a small uncertainty in the mass of the sphere deriving from the fact that in the course of the experiment small pieces of the ecco-foam wall become dislodged and fly off from the sphere, leaving it slightly lighter than it weighed. On the other hand the weight of the glue, which makes the sphere heavier, is also unaccounted for. This error could have been avoided completely by weighing the sphere often in the course of the experiment, but the unavailability of a sensitive scale made this infeasible. Spot checks, however, give the possible mass uncertainty on the order of three milligrams.

Occasional tests, about every fifteen minutes, during the experiment, are made to determine any departure of the speaker behavior from the response measured in the volume calibration. Small changes are observed in the speaker after it has been operated at high volume continuously for over five minutes. The possible error introduced by this variation is about one-tenth of a decibel.

VIII. Departures from Theory and Expected Theoretical Sources of Error

The most obvious point of difference between prediction and observation is that the z planes are not equipotential surfaces. The sphere always remains in contact with the tube wall, from which it cannot be moved, rather than be allowed anywhere in the plane.

The existence of radial forces on nodal-antinodal planes has already been discussed with respect to small particles. The circulation current in this case exists because the walls of the tube are not frictionless as implicitly assumed. Reference to the figures in Section VI, however, shows that the circulation tends to push particles into the center at the velocity antinodes where the sphere is stably held. This suggests that there may be some kind of equilibrium point at the center of the tube. This could be investigated by an experiment designed for that purpose.

Probably the major reason for this behavior is due to the fact, which was ignored in theory, that the presence of the sphere itself causes a major perturbation of the field around it. The scattering effects are calculated by inserting the boundary condition that the component of velocity normal to the ball wall at the ball wall must be zero. The magnitude of the scattering effects is strongly dependant on the size of the ball compared to a wavelength. With a perfect sphere at the exact center, a symmetry situation should exist, again leading to the possibility of stability along the central axis. A slight attraction to the tube wall or a slight irregularity in the shape of the sphere, thus destroying the symmetry, might be responsible for the observed behavior. In the asymmetrical situation, the scattering boundary condition, giving rise to spherical harmonics, will probably result in a net tangential force component. This probably contributes to the tangential forces observed.

In addition to scattering, there is another possible contribution to the other force components. The assumption of an infinitesmally small frequency bandwidth in the theoretical developement contributes to the inability to compute these effects. From equation (12), it is seen that the cylindrical (l,m,n) mode is excited by the frequency $\omega_{l,m,n}$. It was assumed that a driver at frequency $\omega_{0,0,n}$ could be introduced. It is more realistic to assume that a small frequency interval around this frequency is introduced in the driving signal. Between $\omega_{0,0,n}$ and $\Delta\omega$ there may be several $\omega_{l,m,n}$'s

which can excite (l,m,n) modes so that the pressure field in the tube must be expressed in the general form of equation (11) where the coefficients $A_{l,m,n}$ are determined by the spectrum of the incoming signal, the energy available in the system, scattering perturbations, etc. Hitherto it has been assumed that $A_{0,0,n}$ is non-zero and all the other A's are zero. If another $A_{l,n,m}$ is, in fact, appreciably non-zero, then the modes will mix non-linearly by equation (3d), and time average radial and tangential currents will exist in the fluid.

The presence of distortion in the system is another departure from the theoretical model. Though the resonant frequencies associated with the smallest wave numbers constitute the most important contribution to the predicted force by equation (17), the harmonics may get to be large enough to noticeably affect the behavior of the system. The effects of each harmonic cannot be accounted for by simple superposition due to the non-linearity of the second order, but the complete first order expression, $\sum_t p_{0,0,tn}$, can be inserted into equation (3d) to get a second order expression.

The theory also differs from the actual experiment in the fact that the balls used are not exactly spherical. The asymmetry introduced by this condition has already been discussed. It is possible of course, to solve for the force due to field pressure on any shape obstacle by numerical means. A better approximation to the experiment, for example, might be to integrate over the surface of an ellipsoid. The integrals in this calculation are not readily calculable in exact form, but may be done by these means.

Finally, the assumption of a rigid walled cavity is not realized due, for the most part, to the presence of the speaker, which is set into the tube wall. This causes small eddy current disturbances which die out far from the speaker. For this reason, the data is taken in the topmost node, as far from the speaker as possible.

IX. Results and Discussion

The aim of this experiment is, in part, to check the validity of the expression for the force on a sphere given by equation (17). At the minimum suspending volume, we expect the condition

$$\langle F_z \rangle_{max} = mg \tag{19}$$

where m is the mass of the sphere and g, the acceleration due to gravity. The maximum value of $\langle F_z \rangle$ occurs at those values of z such that $\sin \frac{2n\pi z}{L} = \pm 1$. The condition for stability, $\langle F_z \rangle'' < 0$, (primes signify differentiation with respect to z), is met for $\sin \frac{2n\pi z}{L} = +1$. Thus, if $\langle F_z \rangle_{max}$ is greater than the gravitational force on the sphere, mg, then there will be stable points of suspension at a distance apart of one half of the wavelength associated with the linear wave. This prediction is verified by the data of Appendix III B.

More quantatively, at minimum suspending volume, $A_{n,min}$ in the notation of equation (17), the suspension condition is

$$mg = \frac{A_{n,min}^2}{2\rho_0 c^2 n} \left[\frac{L}{2n\pi a} \sin \frac{2n\pi a}{L} - \cos \frac{2n\pi a}{L} \right] \tag{20}$$

The experimental data pertaining to equation (20) is given in Appendix III C in graph form. For each sphere used, there are three graphs plotted:

1. Minimum suspending R.M.S. voltage vs. sphere mass
2. Minimum suspending decibel level vs. $\log_{10}$ sphere mass
3. Minimum suspending R.M.S. voltage vs. wave number, n

A. The Mass-Pressure Dependence

Since there is a linear microphone relationship between voltage of the output signal and the sound pressure amplitude, A_n, graph (1) for each sphere should, by equation (20), have a quadratic form at each resonance frequency. The exponential dependence of the plots in graphs (1) is seen in the log-log graphs (2).

In graphs (2)

$$L\ (db) = 20 \log_{10} \left(\frac{A_n}{P_0} \right) \quad ; P_0 = 2 \times 10^{-4} \text{ dynes/cm}^2$$

$$\log_{10} m_{re\ 100\ mg} = \log_{10} \left(\frac{m}{m_0} \right) \quad ; m_0 = 100 \text{ milligrams}$$

Writing a general exponential relationship

$$\frac{m}{m_0} = K\left(\frac{A_n}{P_0}\right)^s \qquad (21)$$

and taking the log of both sides

$$\log_{10}\left(\frac{m}{m_0}\right) = \log_{10} K + s\log_{10}\left(\frac{A_n}{P_0}\right) \qquad (22)$$

The straight lines of graphs (2) are of the form

$$20\log_{10}\left(\frac{A_n}{P_0}\right) = j\log_{10}\left(\frac{m}{m_0}\right) + b$$

where j is the slope of the line and b the y intercept. Combining (21) and (22),

$$K = 10^{-b/j} \quad ; \quad s = 20/j \qquad (23a,b)$$

Values of 20/j and b/j are given in graphs (2) for each line plotted.

The error bars in graphs (2) represent roughly the spread of the four or five values taken for each point around the mean of these values. The major sources of these errors are those discussed under the heading of experimental difficulties.

If expression (20) is an accurate description, s should equal two. This value is seen to be well within the range of possible values as determined by the limited accuracy of measurement in most of the plots. The fact that s = 2 is approached closely in the most consistent, lowest error, graphs of spheres (1) and (3) gives credibility to the possible significance of that value.

B. Pressure- Wave Number Dependence

In the experiment the sphere radii used are less than or equal to 1.7 cm. Thus, the quantity $\frac{2n\,a}{L} \lesssim \frac{n}{18}$ is small enough to allow an expansion of the sines and cosines in equation (20) to give

$$mg = 2A_{n,m,n}^2 \pi^2 a^3 n / L\rho_0 c^2 \qquad (24)$$

For a constant mass, equation (24) shows a linear relationship between the square of the pressure amplitude and the reciprocal of the wave number.

Graphs (3) bear out this linear dependence for the small number of points plotted. The ordinate of these graphs is the ratio of the pressure amplitude at the n^{th} resonance to that of the n=10 resonance, quantity squared. The points are determined by the mean decibel difference between the lines of graphs (2) where

$$\Delta L_n(dB) = L_n - L_{10} = 20\log\frac{A_n}{A_{10}} = 10\log\left(\frac{A_n}{A_{10}}\right)^2$$

giving: $$\left(\frac{A_n}{A_{10}}\right)^2 = 10^{\Delta L_n/10} \quad .$$

The error bars in graphs (3) are found by the possible error in L_n due to the errors in graphs (2).

C. The Magnitude of the Force

As a further test for the validity of equation (20), we compare the measured magnitude of the force to that predicted. Using equation (24), the small sphere approximation to (20), and equations (21) and (23a) gives

$$K = 10^{-b/j} = 2\pi^2 a^3 n P_0^2 / g L \rho_0 c^2 m_0 \qquad (25)$$

$$b/j = \log_{10}\left[g L \rho_0 c^2 m_0 / 2\pi^2 a^3 n P_0^2\right]$$

Using parameter values which represent the average experimental situation, a=1 cm, n = 6, L = 200 cm, b/j, computed from (25) is 15.72 which compares very favorably to the data of Appendix III C.

D. Pressure-Diameter Dependence

In graph (4) of Appendix III C, the log of the pressure (decibel level) is plotted against the log of the average radius of the spheroid. The points on this graph are gotten by plotting the y intercepts of graphs (2) against the log of the spheroid average radius divided by 1.025 cm., the average radius of the smallest spheroid.

Equation (24) predicts that at constant mass, $A_n \propto a^{-3/2}$. From this dependence the slope of the log-log line is expected to be-30. The experimental values, given in graph (4), do not agree very well with prediction. Further, the points cannot be well approximated by a straight line fit of any kind.

This disagreement indicates that there is another parameter involved in this relationship. This is not surprising due to the fact that the spheroids are actually ellipsoids of different eccentricities, a situation unlike the theoretical assumption behind equation (24). Thus, it is reasonable to assume that the pressure is a function of both size (length of axes) and also shape (eccentricity).

Appendix I [6]

Microphone Characteristics

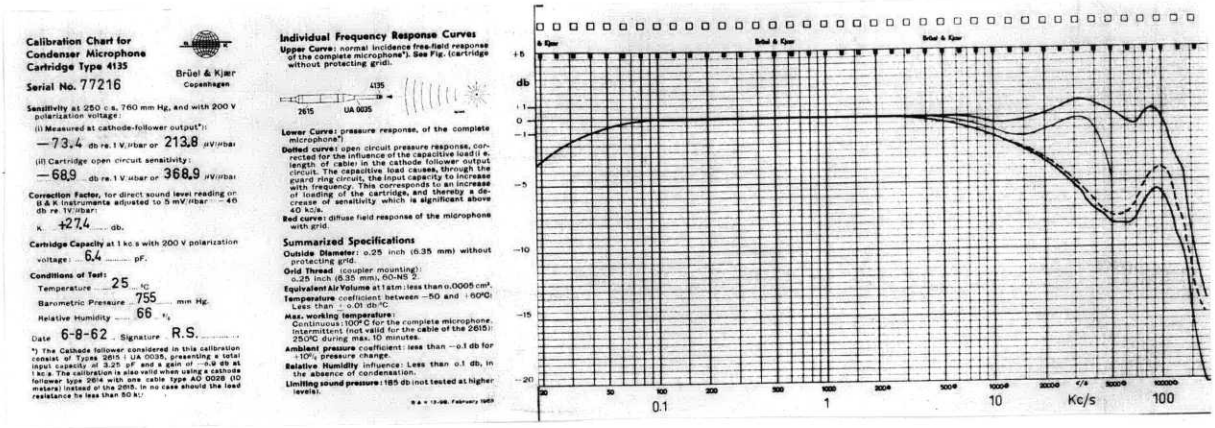

Calibration Chart for Condenser Microphone Cartridge Type 4135

Brüel & Kjær Copenhagen

Serial No. 77216

Sensitivity at 250 c.s, 760 mm Hg, and with 200 V polarization voltage:

(i) Measured at cathode-follower output*):
−73.4 db re. 1 V/μbar or 213.8 μV/μbar

(ii) Cartridge open circuit sensitivity:
−68.9 db re. 1 V/μbar or 368.9 μV/μbar

Correction Factor, for direct sound level reading on B & K instruments adjusted to 5 mV/μbar: −46 db re. 1V/μbar:
K +27.4 db.

Cartridge Capacity at 1 kc.s with 200 V polarization voltage: 6.4 pF.

Conditions of Test:
Temperature 25 °C
Barometric Pressure 755 mm Hg.
Relative Humidity 66 %
Date 6-8-62. Signature R.S.

*) The Cathode follower considered in this calibration consist of Types 2615 + UA 0035, presenting a total input capacity of 3.25 pF and a gain of −0.9 db at 1 kc.s. The calibration is also valid when using a cathode follower type 2614 with one cable type AO 0028 (10 meters) instead of the 2615. In no case should the load resistance be less than 50 kΩ.

Individual Frequency Response Curves

Upper Curve: normal incidence free-field response of the complete microphone*). See Fig. (cartridge without protecting grid.

4135
2615 UA 0035

Lower Curve: pressure response, of the complete microphone*)

Dotted curve: open circuit pressure response, corrected for the influence of the capacitive load (i.e. length of cable) in the cathode follower output circuit. The capacitive load causes, through the guard ring circuit, the input capacity to increase with frequency. This corresponds to an increase of loading of the cartridge, and thereby a decrease of sensitivity which is significant above 40 kc/s.

Red curve: diffuse field response of the microphone with grid.

Summarized Specifications

Outside Diameter: 0.25 inch (6.35 mm) without protecting grid.

Grid Thread (coupler mounting): 0.25 inch (6.35 mm), 60-NS 2.

Equivalent Air Volume at 1 atm: less than 0.0005 cm³.

Temperature coefficient: between −50 and +60°C: Less than ± 0.01 db/°C.

Max. working temperature: Continuous: 100°C for the complete microphone. Intermittent (not valid for the cable of the 2615): 250°C during max. 10 minutes.

Ambient pressure coefficient: less than −0.1 db for +10% pressure change.

Relative Humidity influence: Less than 0.1 db, in the absence of condensation.

Limiting sound pressure: 185 db (not tested at higher levels).

B & K 12-62. February 1962

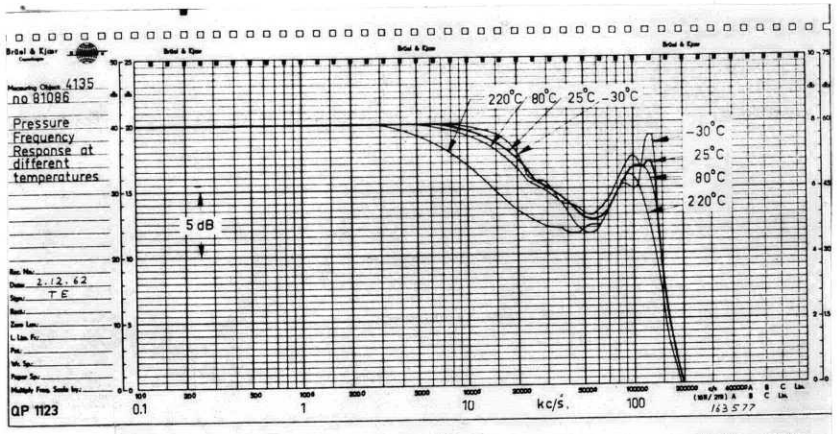

Influence of temperature on the frequency response of the 4135.

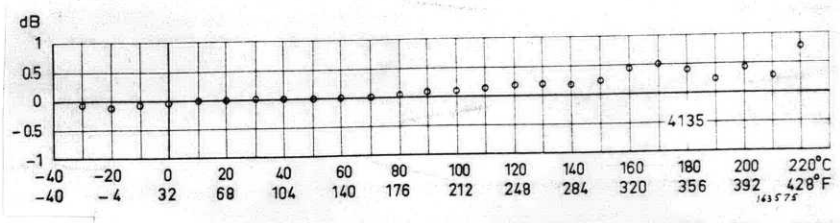

Typical sensitivity versus temperature check on a cartridge Type 4135 at 1000 c/s.

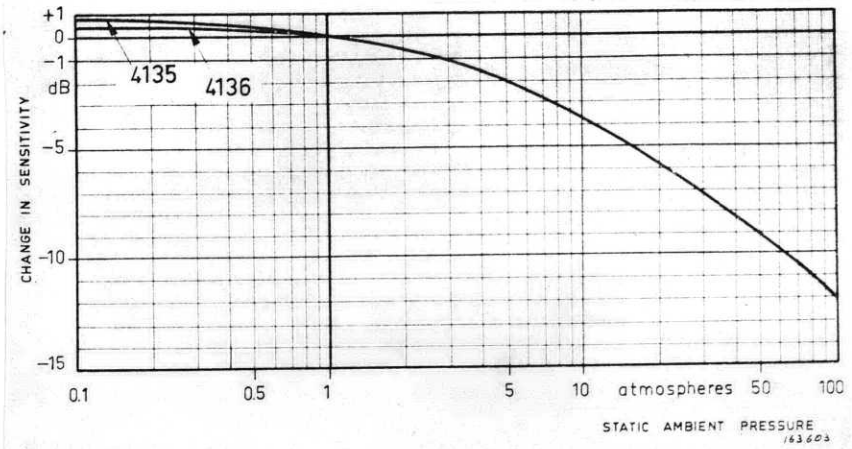

Fig. 25. Variation of the quarter-inch microphone sensitivity as a function of the static ambient pressure. Measurements made down to 14 mmHg (0.02 atm., or 26 Km - 86000 ft. altitude) show that the sensitivity in vacuum would be less than 1 dB higher than the sensitivity at 1 atm.

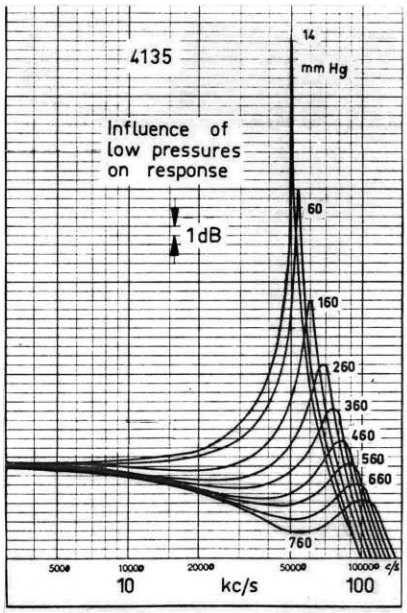

Fig. 26. Influence of the static ambient pressure on the frequency response of the quarter-inch microphones.

Appendix II

Patterns Made by Particles in Cavity

#1. Tube horizontal
573 cps., 152 db

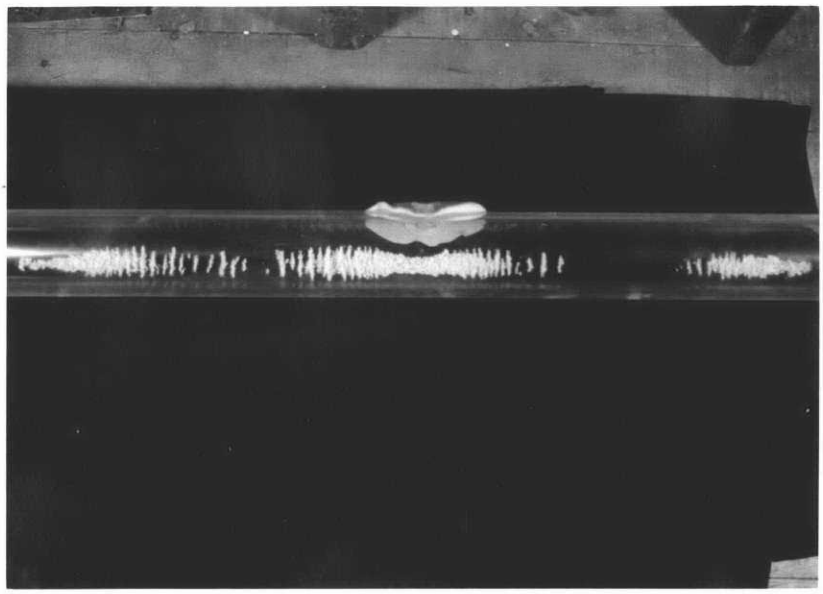

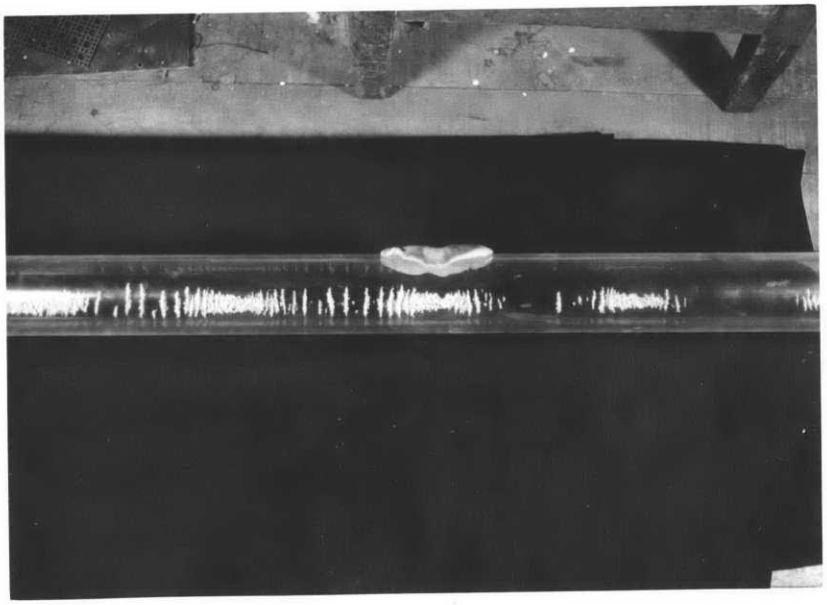

#2. Tube Horizontal
955 cps., 157 db

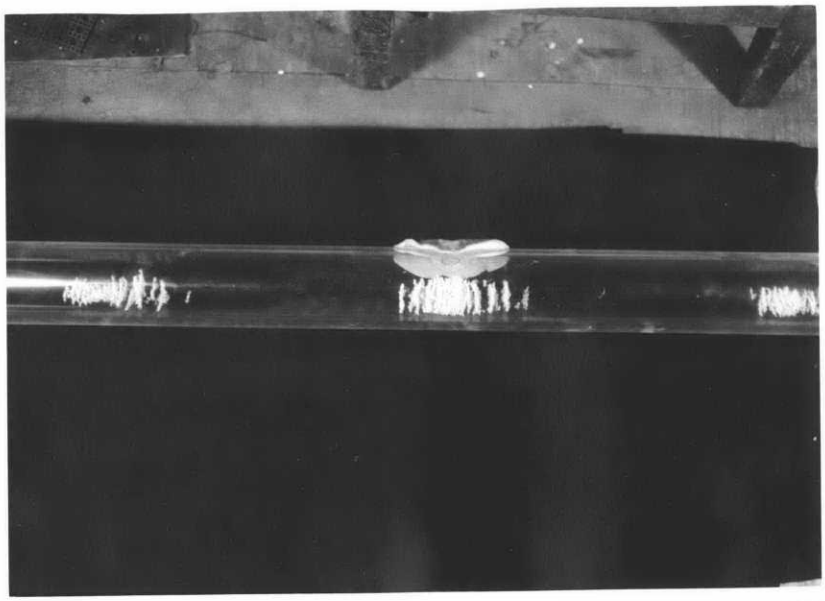

#3. Tube Horizontal
573 cps., 160 db.

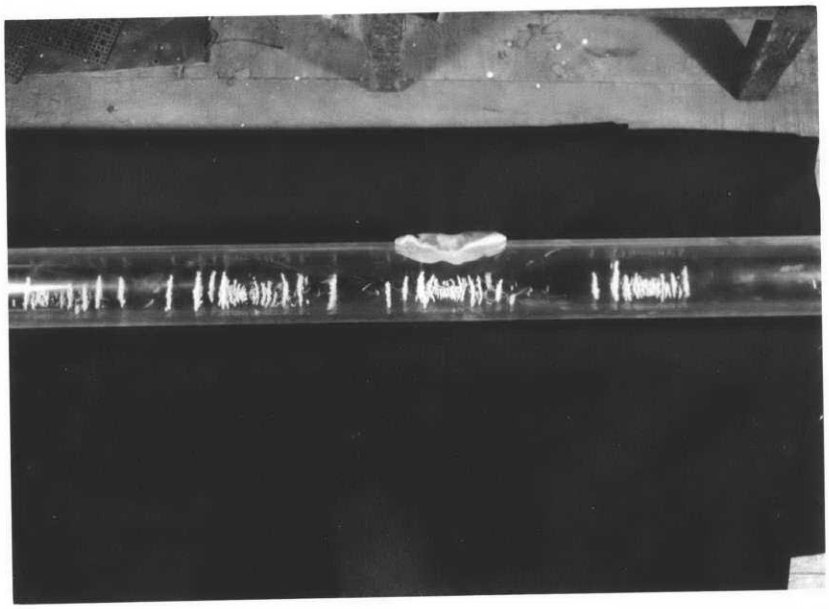

#4. Tube Horizontal
955 cps., 163 db

#5. Tube Horizontal
955 cps., 163 db
Close-up on Nodal
Eye

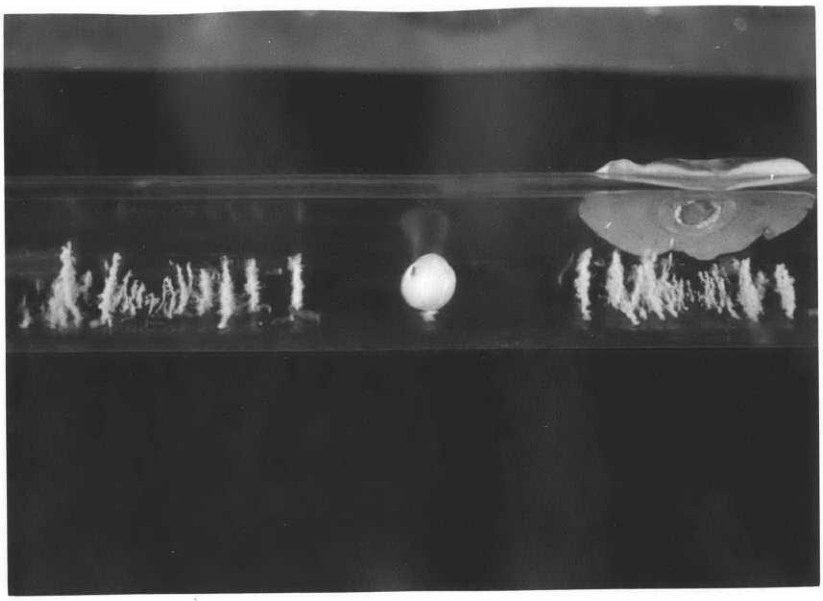

#6. Tube Horizontal
764 cps., 164 db
Sphere and Particles

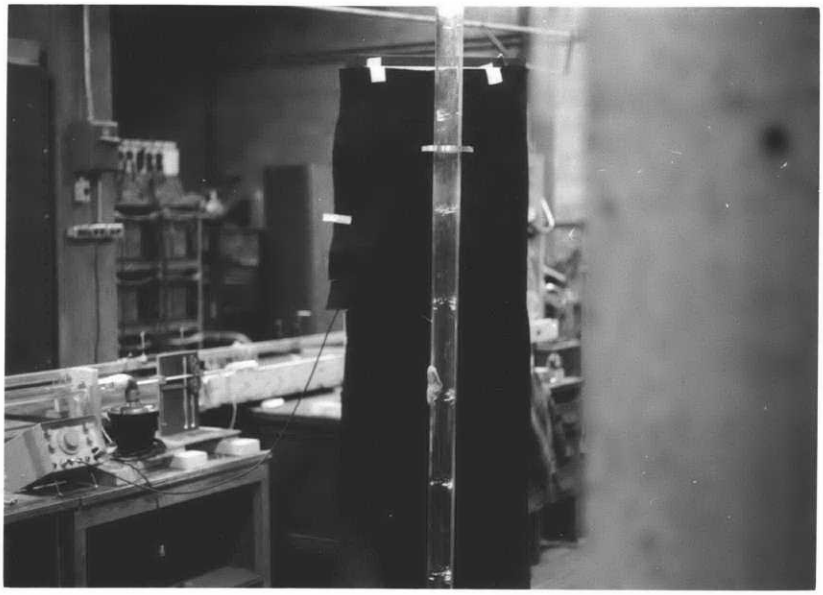

#7. Tube Vertical
764 cps., 164 db.

#8. Tube Vertical
764 cps., 164 db
Close-up of Node
from Top

#9. Tube Vertical
764 cps., 164 db
Close-up of Node
from Side

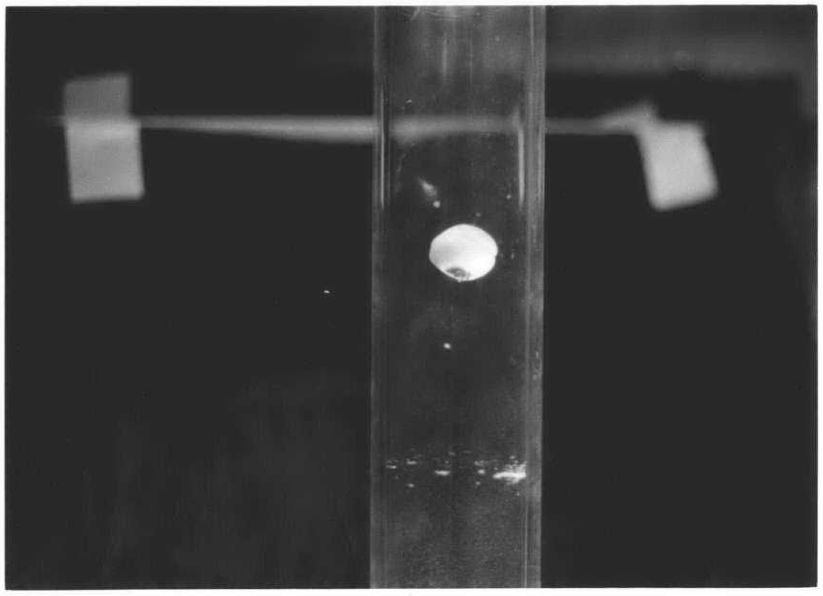

#10. Tube Vertical
764 cps., 164 db
Suspended Sphere

Appendix III A

Resonant Frequencies of the Resonant Cavity

f (cps)	$\Delta f = f_n - f_{n-1}$	n
191		2
	96	
287		3
	96	
383		4
	95	
478		5
	95	
573		6
	96	
669		7
	95	
764		8
	95	
859		9
	96	
955		10
	95	
1050		11

$f_n = \omega_n/2\pi = nc/2L$

$\Delta f = c/2L \quad 95.5 \quad L = 174$ cm Direct Measurement = 175 ± 3

Appendix III B

Location of Nodes in the Cavity

f = 764 n = 8 Linear wavelength λ = 43.3 cm.

All measurements from the top of the tube

Node #	$\underline{z}$ (vertical displacement from top)	$\Delta \underline{z} = \underline{z}_n - \underline{z}_{n-1}$
1	17	21
2	38	22
3	60	21
4	81	22
5	103	22
6	125	20
7	145	22
8	167	

f = 573 n = 6 Linear Wavelength λ = 57.8 cm.

All measurements from the top of the tube

Node #	$\underline{z}$ (vertical displacement from top)	$\Delta \underline{z} = \underline{z}_n - \underline{z}_{n-1}$
1	22	31
2	53	28
3	81	29
4	110	28
5	138	28
6	166	

Appendix III C

Experimental Data

Ball #1

Graph (1)

Ave Diam = 3.20 cm.

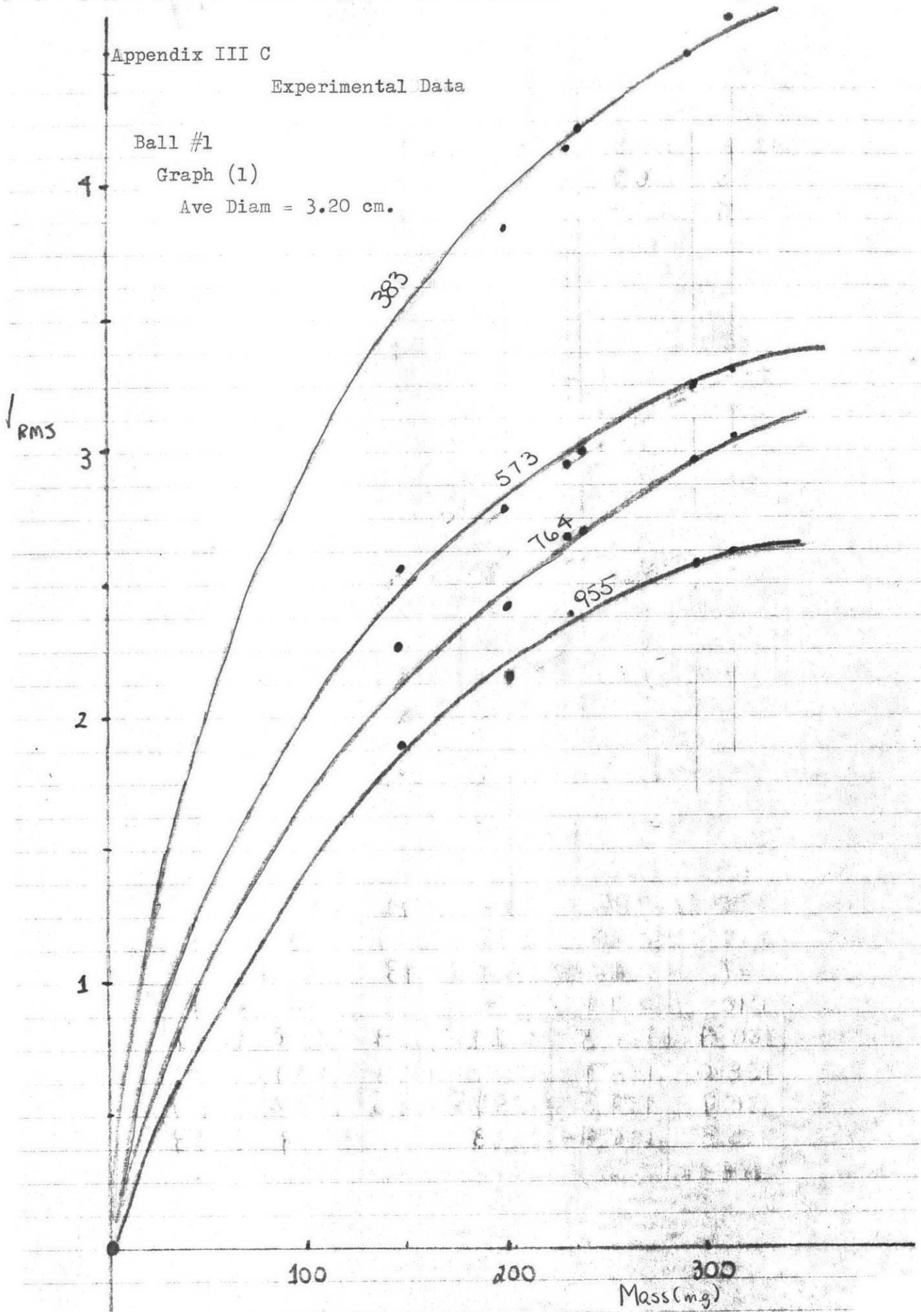

Ball #1
Graph (2)

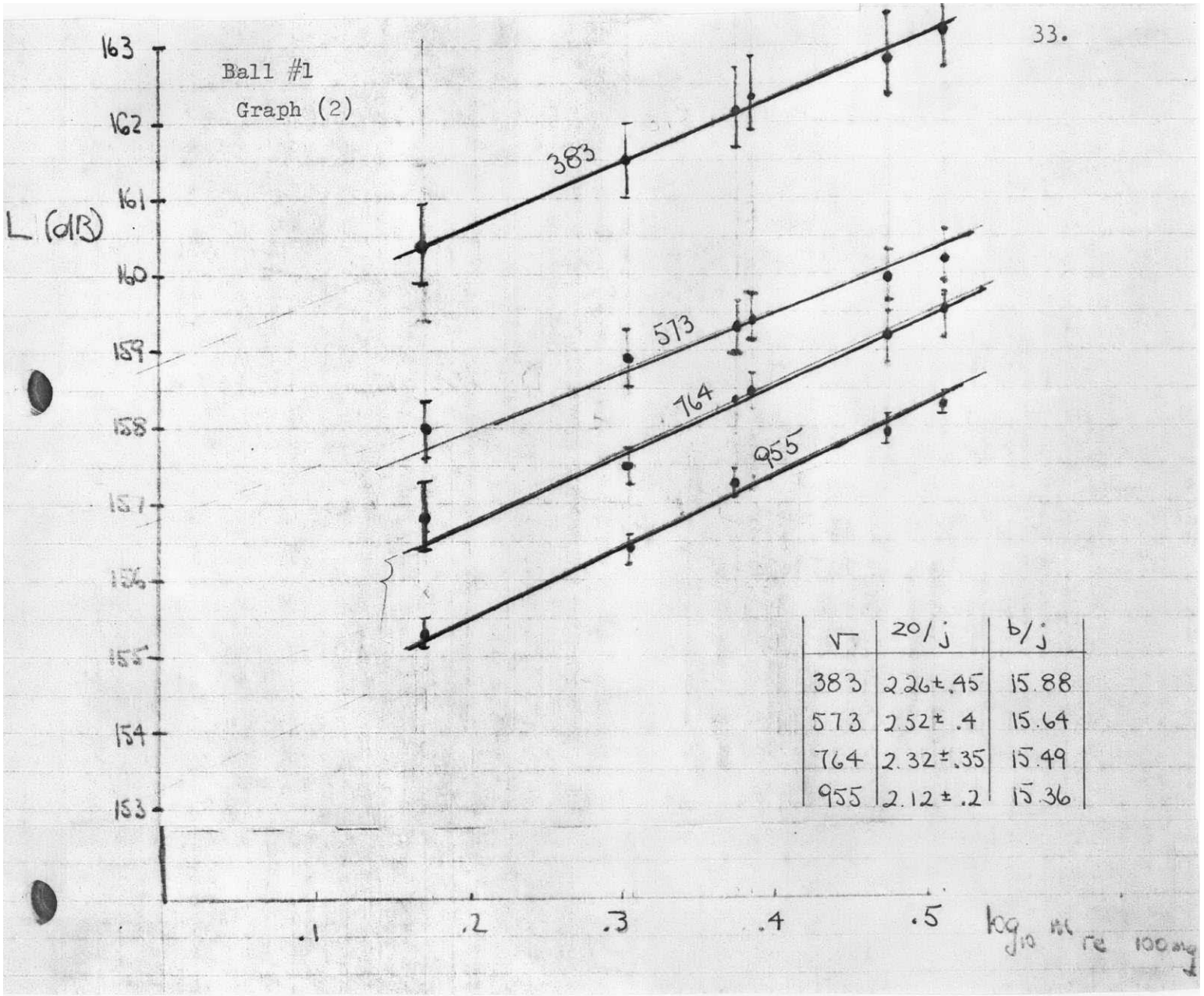

ν	20/j	b/j
383	2.26 ± .45	15.88
573	2.52 ± .4	15.64
764	2.32 ± .35	15.49
955	2.12 ± .2	15.36

Ball #1
Graph (3)

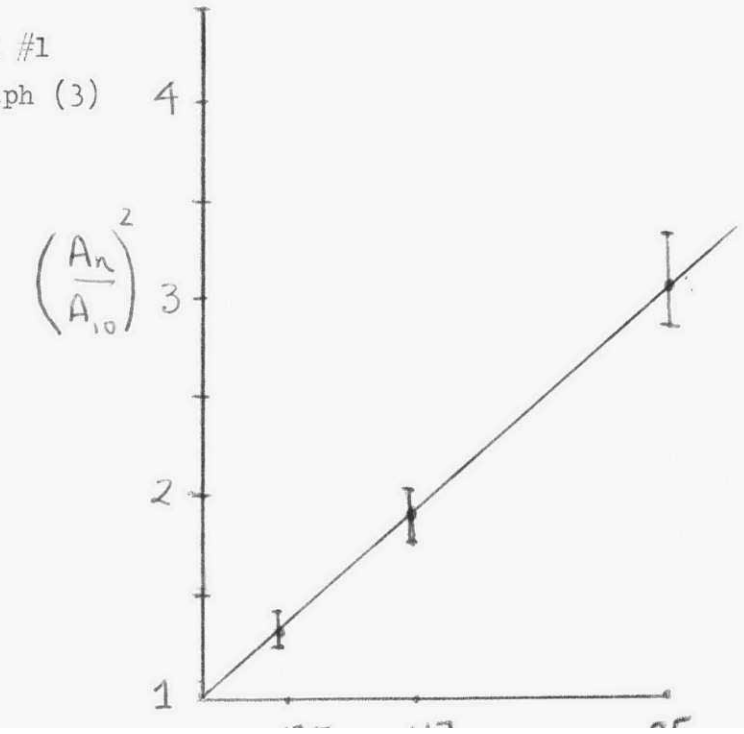

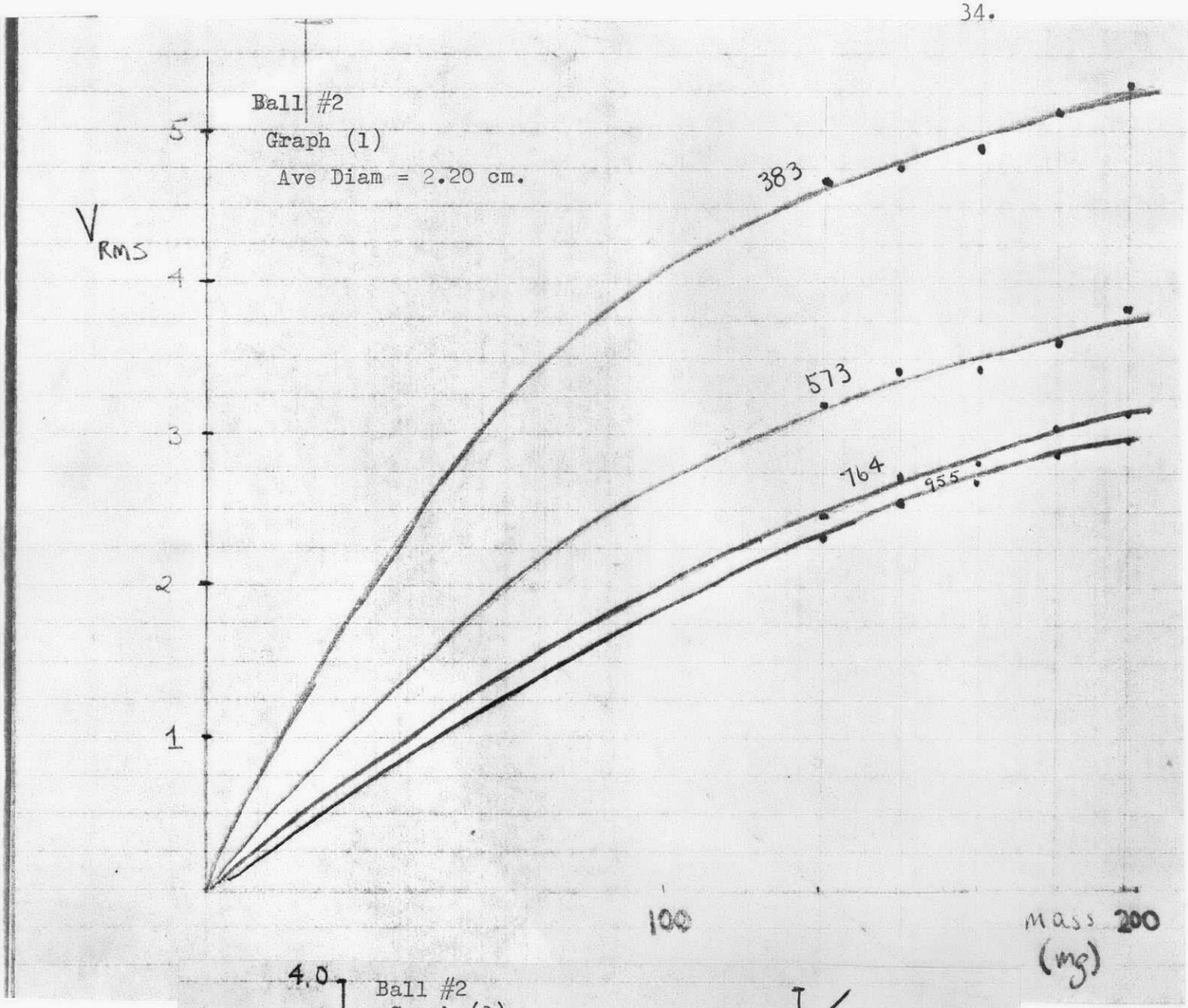
Ball #2
Graph (1)
Ave Diam = 2.20 cm.
V_{RMS}
5
4
3
2
1
383
573
764
955
100
200
mass
(mg)

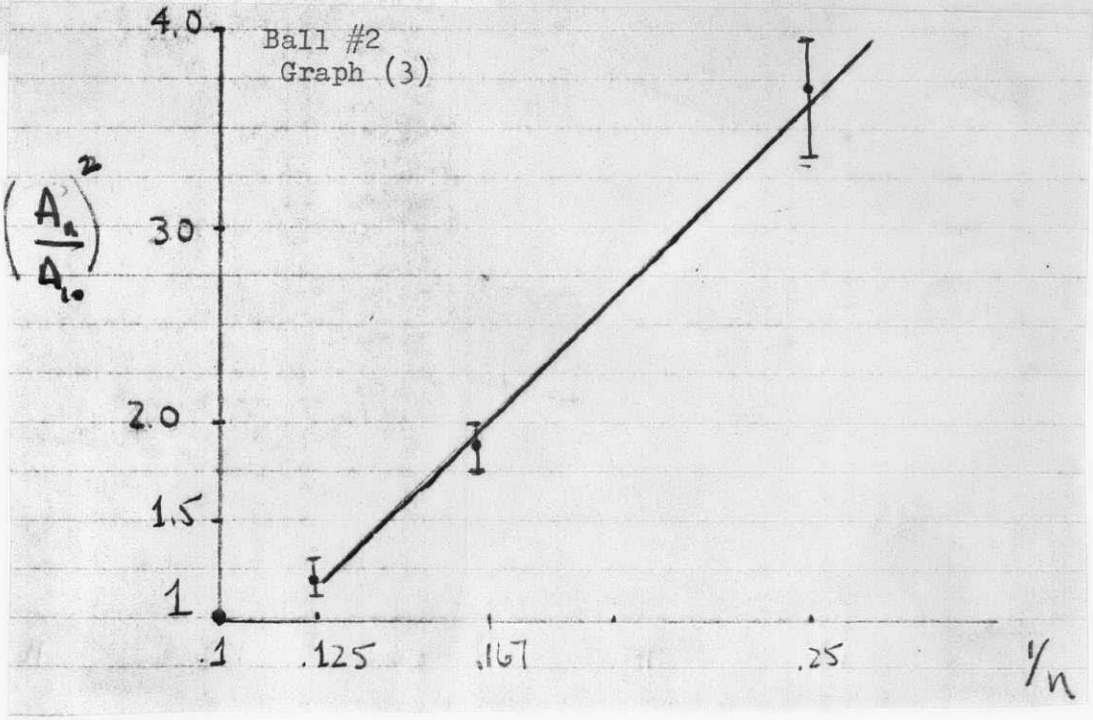
Ball #2
Graph (3)
$\left(\frac{A_n}{A_1}\right)^2$
4.0
3.0
2.0
1.5
1
.1
.125
.167
.25
1/n

Ball #2
Graph (2)

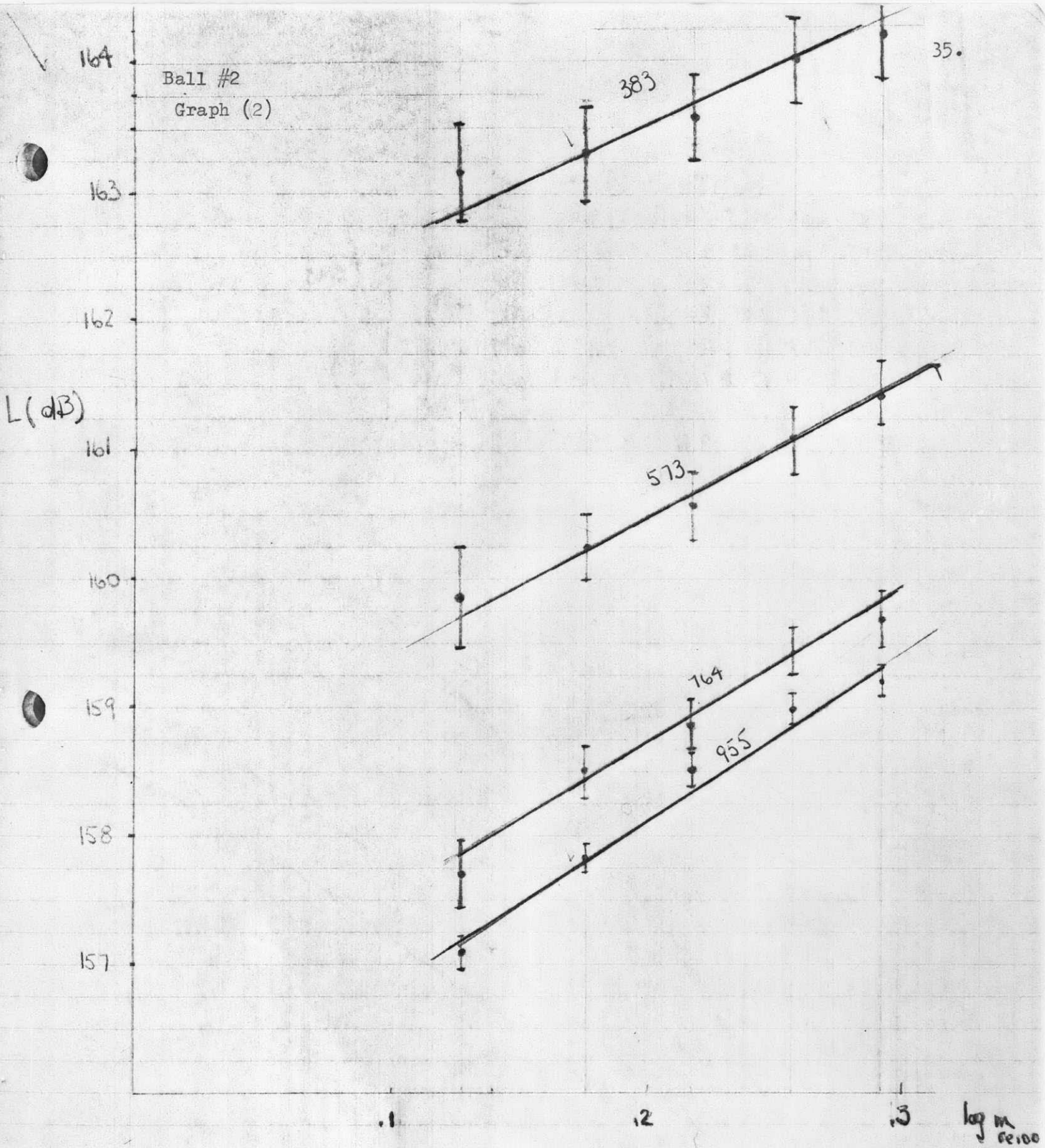

v	20/j	b/j
383	2.35 ± 1	16.17
573	1.72 ± .6	15.82
764	1.66 ± .5	15.63
955	1.58	15.56

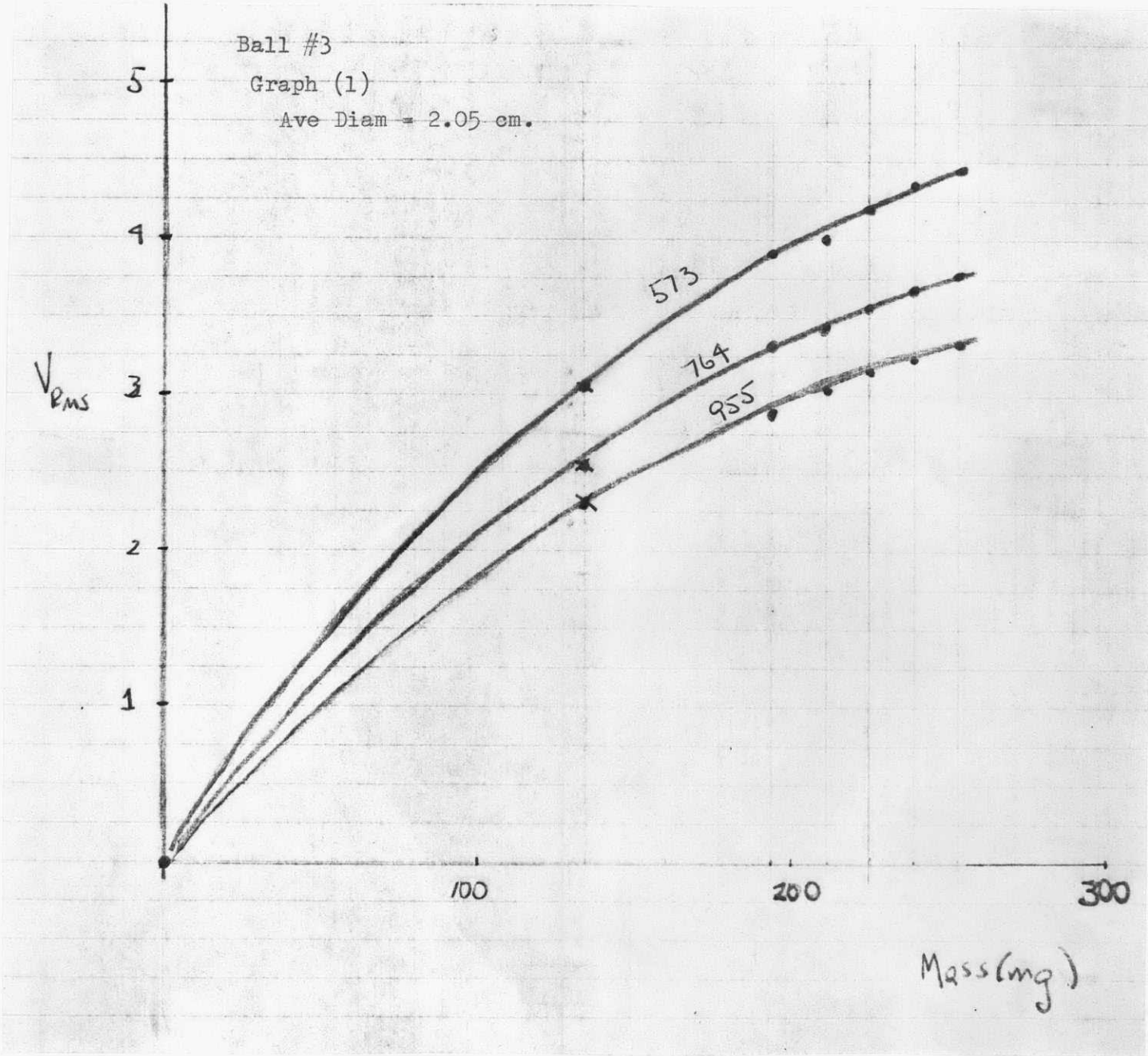
Ball #3
Graph (1)
Ave Diam = 2.05 cm.
5
4
3
2
1
V_{RMS}
573
764
955
100
200
300
Mass (mg)

Ball #3
Graph (2)

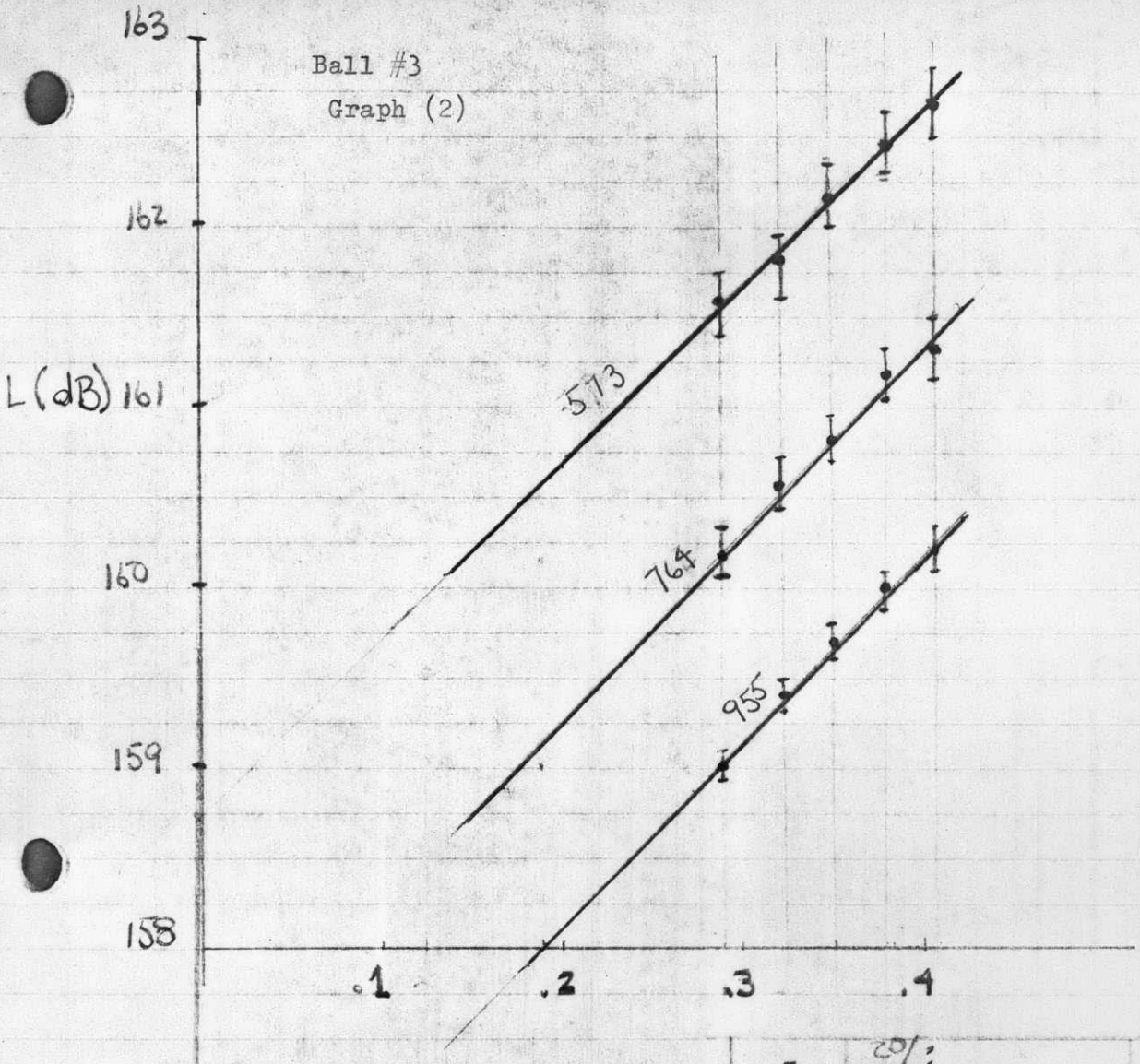

r	a/j	b/j
955	2.00 ± .25	15.61
764	1.93 ± .3	15.71
573	2.16 ± .4	15.88

Ball #3
Graph (3)

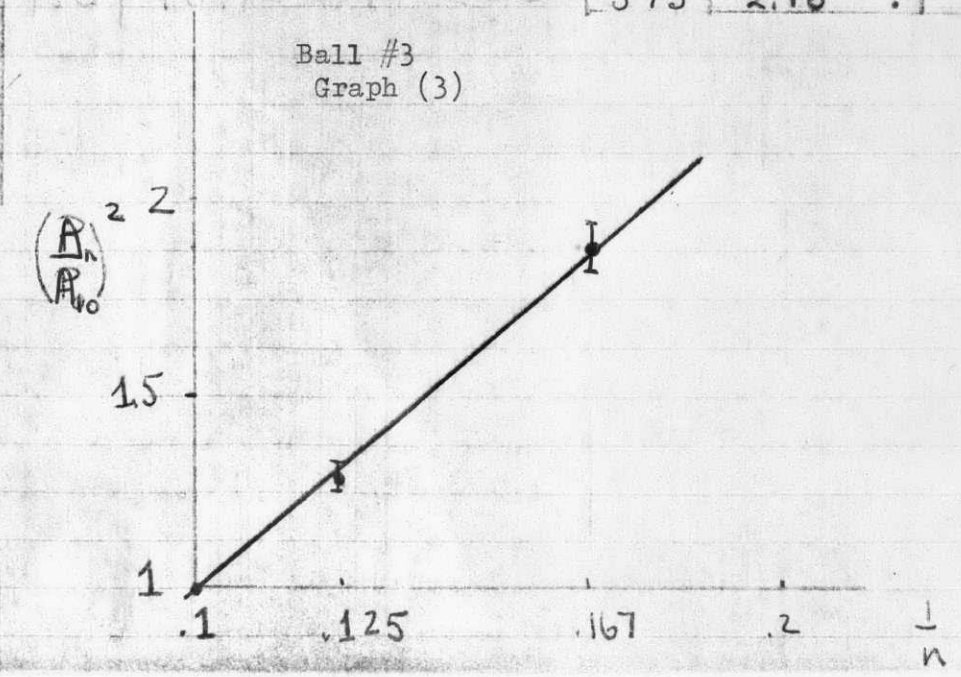

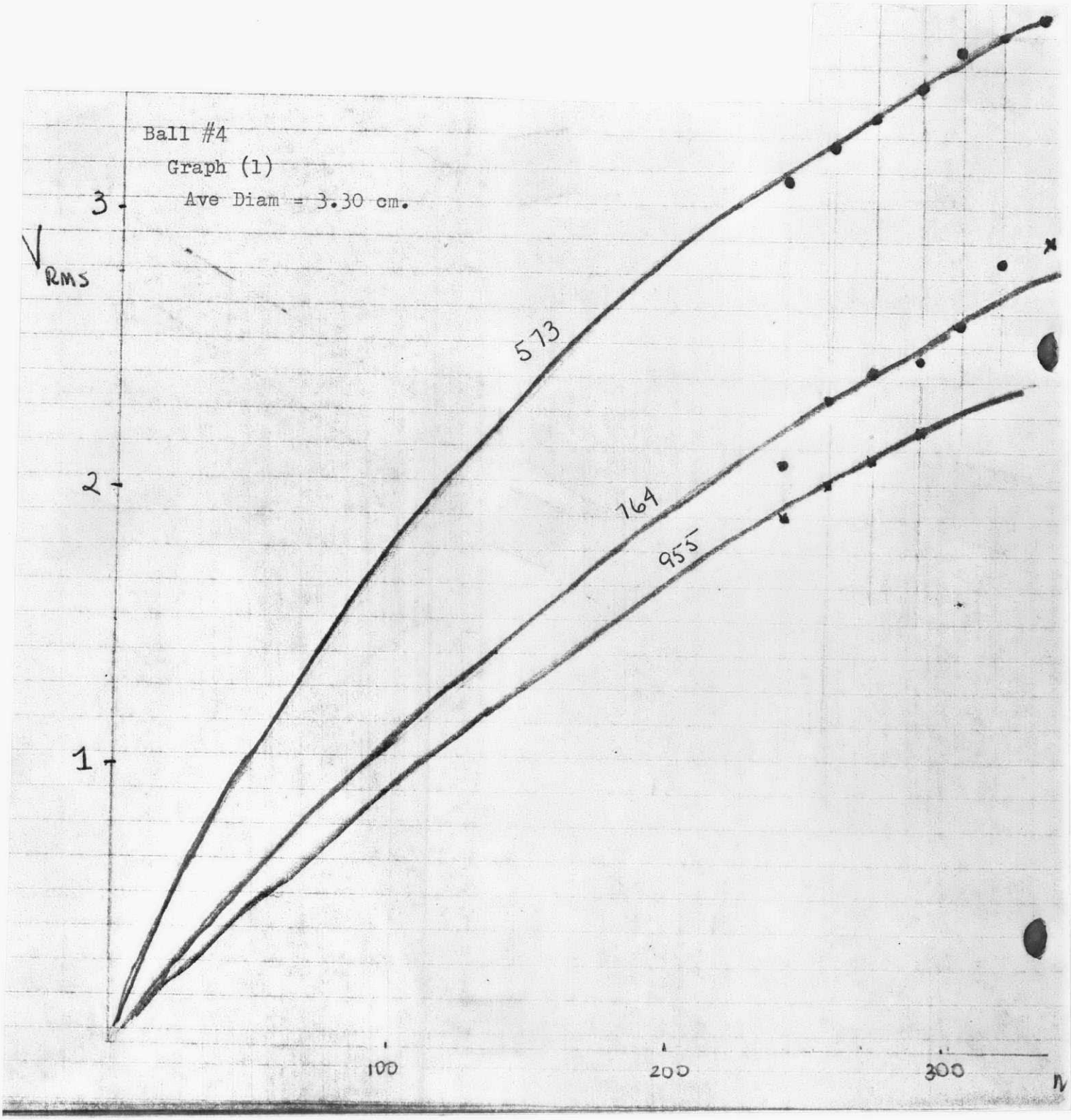
Ball #4
Graph (1)
Ave Diam = 3.30 cm.
3
2
1
V RMS
573
764
955
100
200
300
N

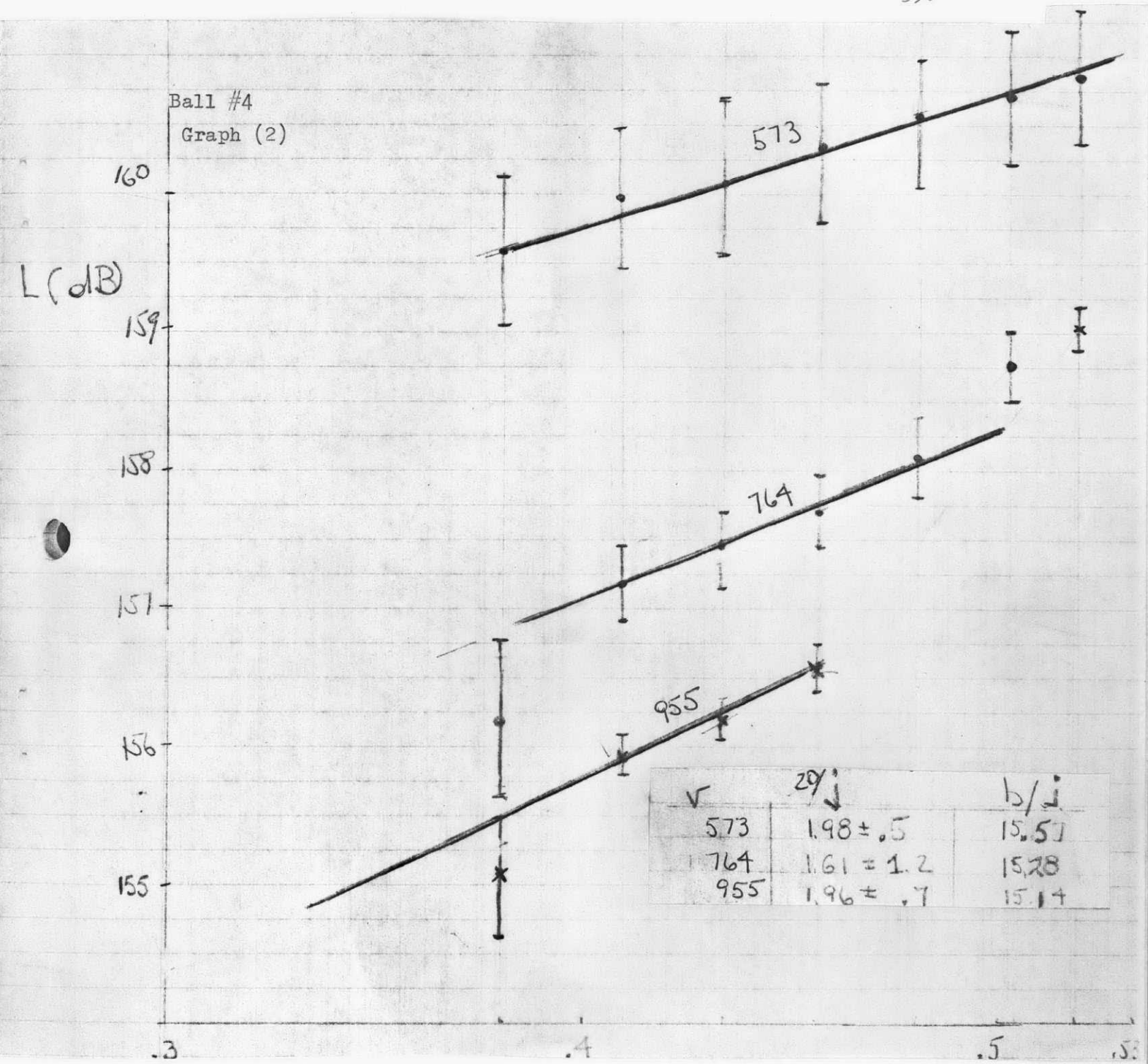

ν	2σ/j	b/j
573	1.98 ± .5	15.51
764	1.61 ± 1.2	15.28
955	1.96 ± .7	15.14

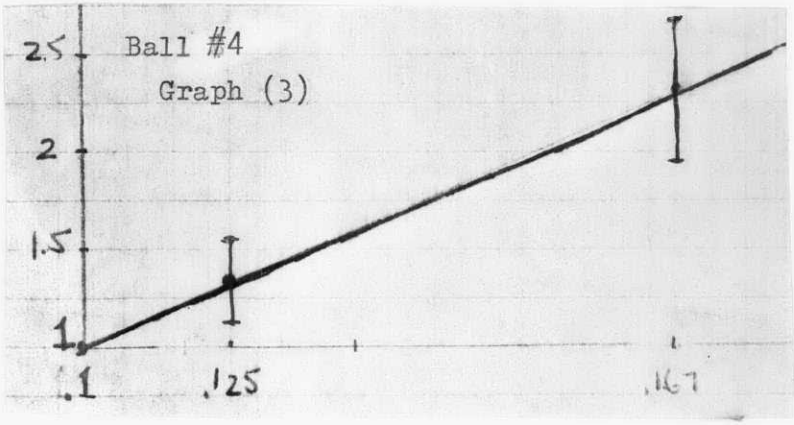

Graph (4)

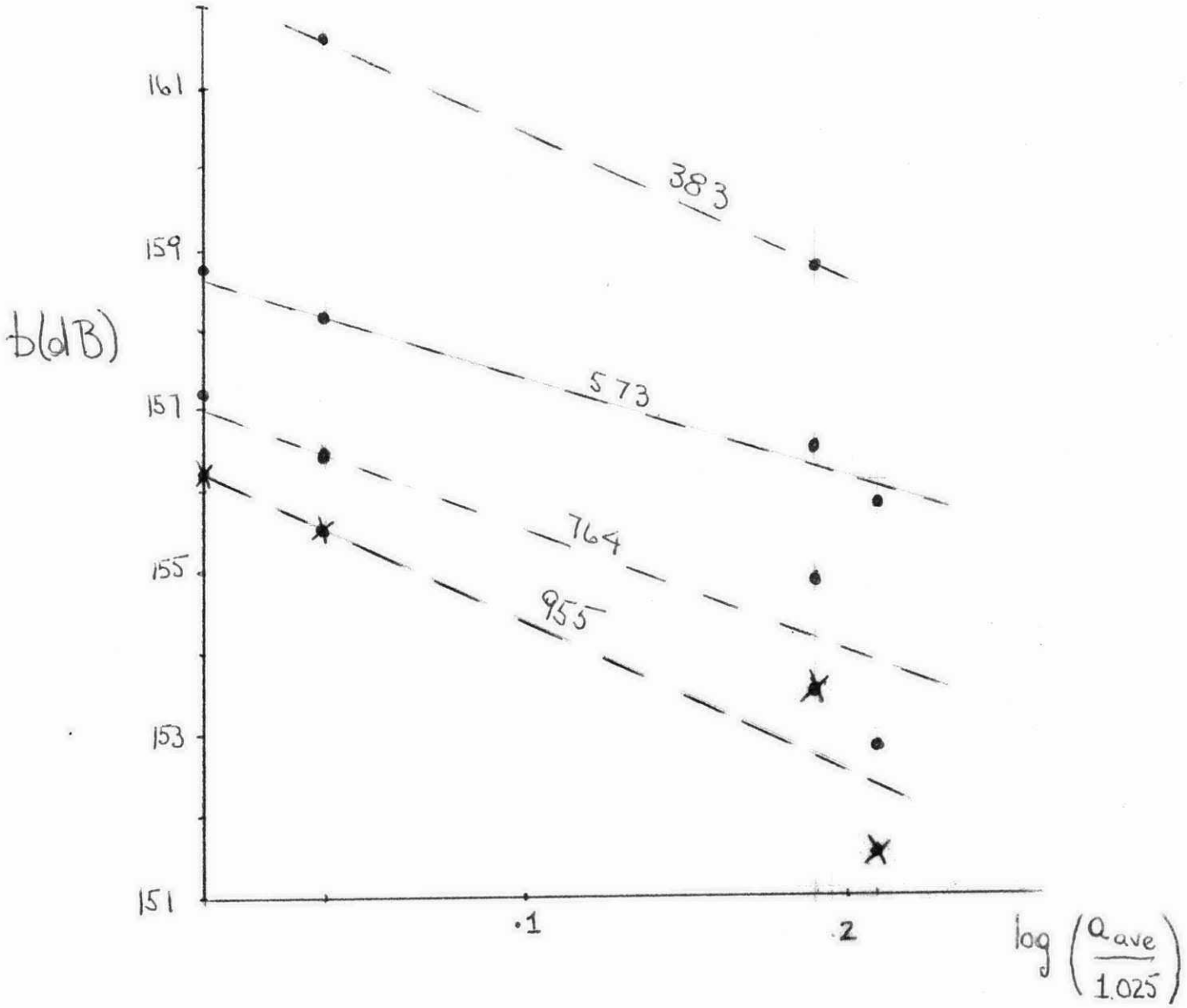

$S_{383} = -1.8$

$S_{573} = -1.18$

$S_{764} = -1.32$

$S_{955} = -2.06$

Appendix IV

Harmonic Distortion Curves

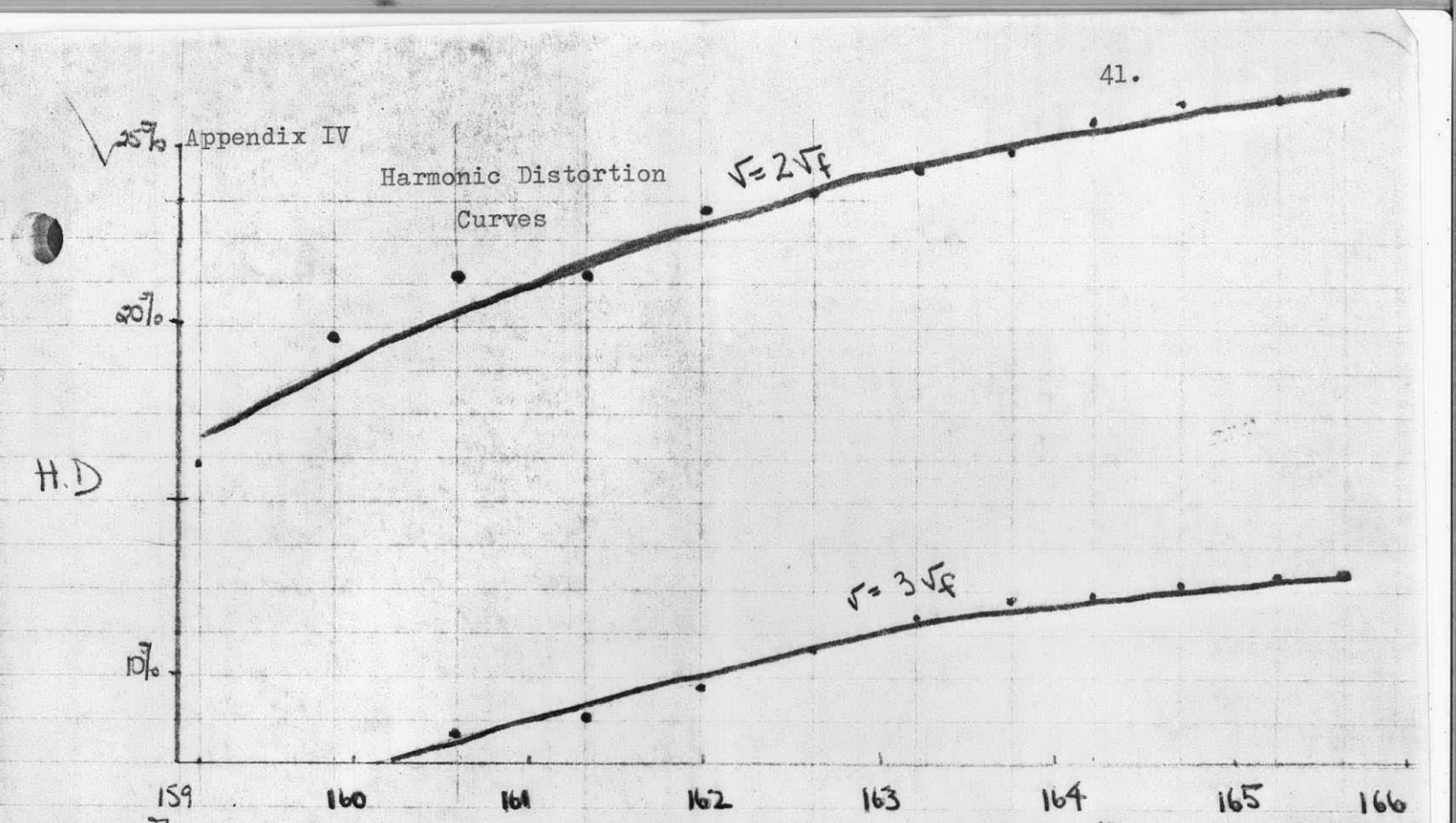

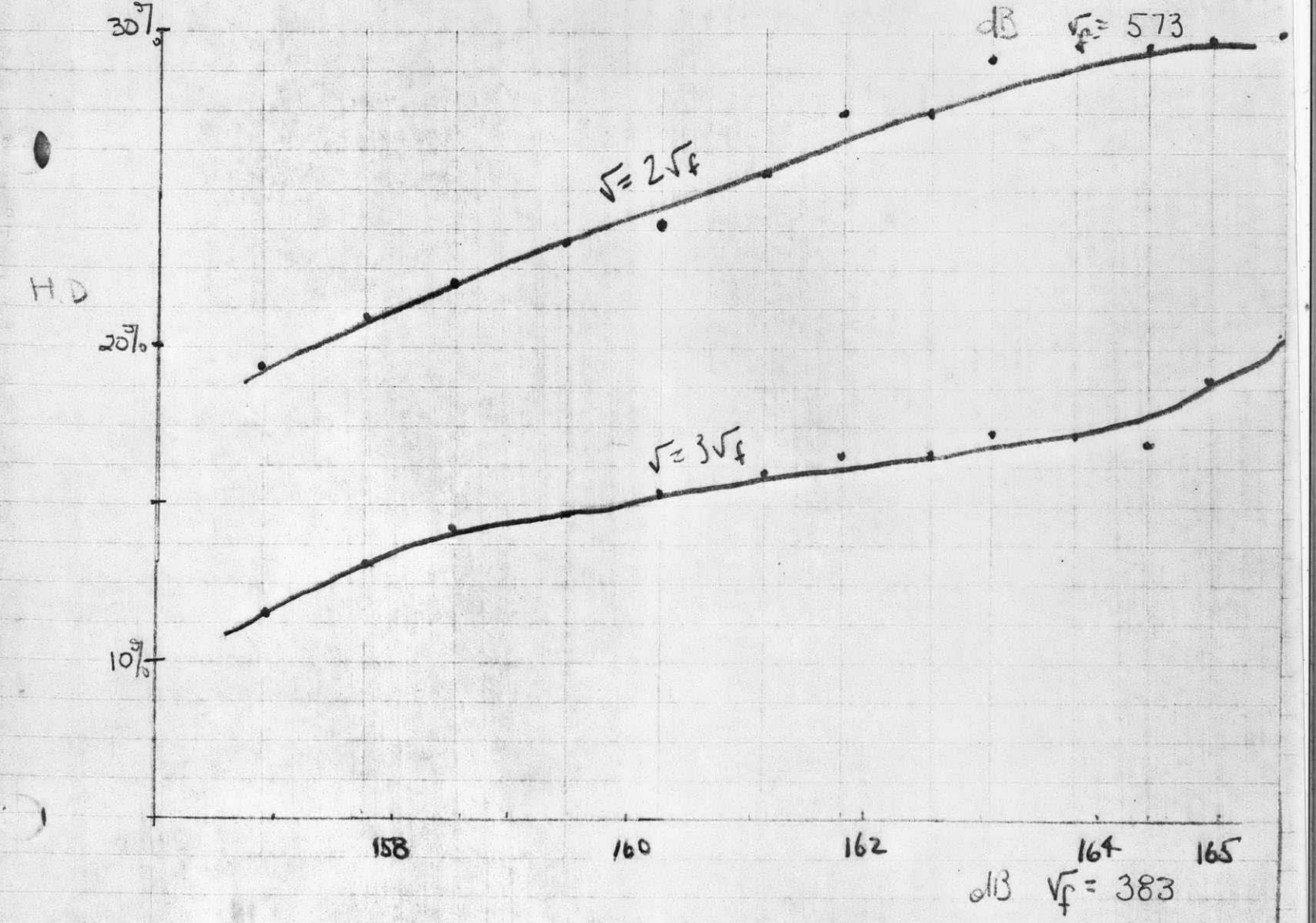

Harmonic Distortion Curves for Atlas Speaker

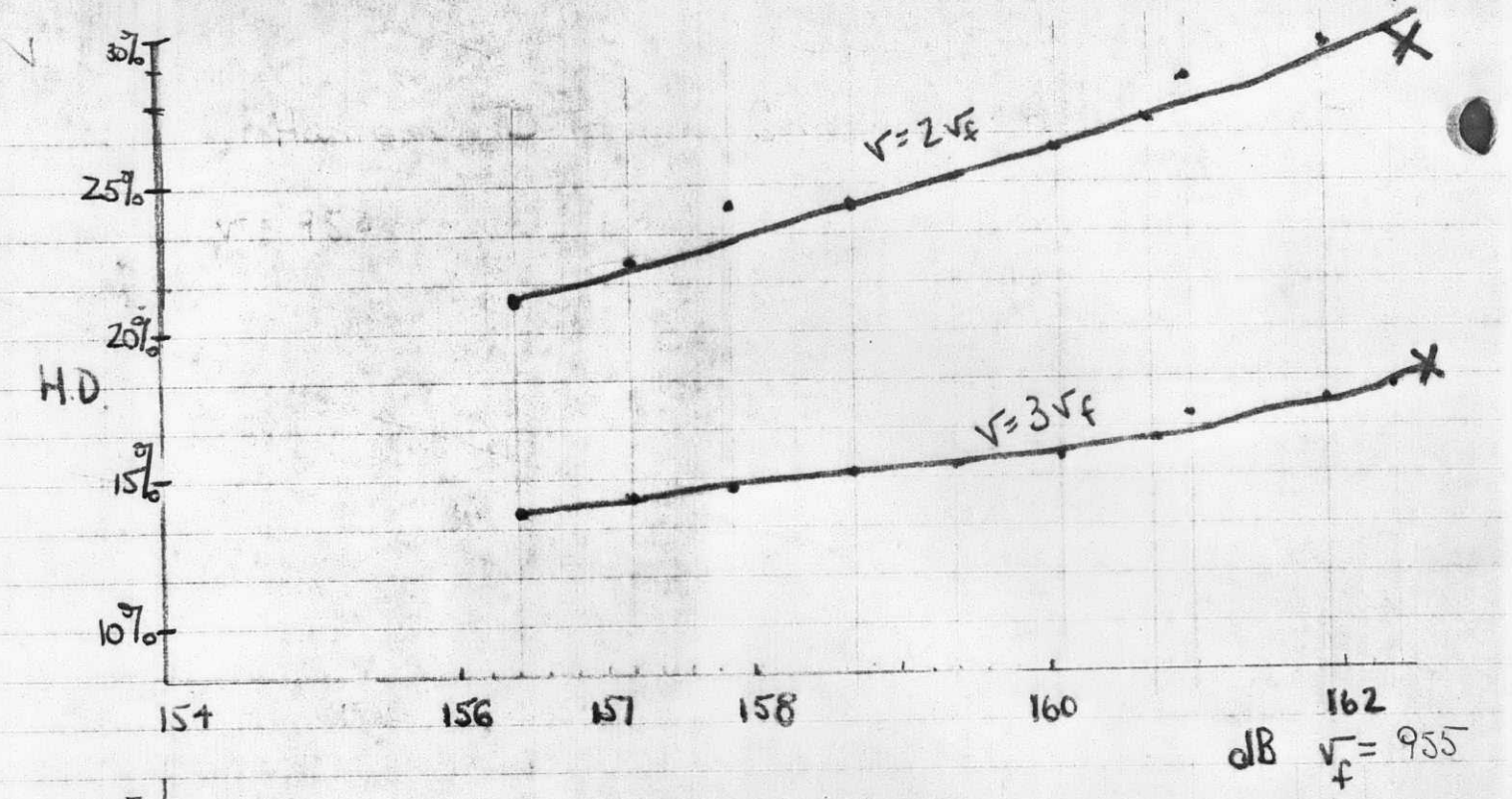

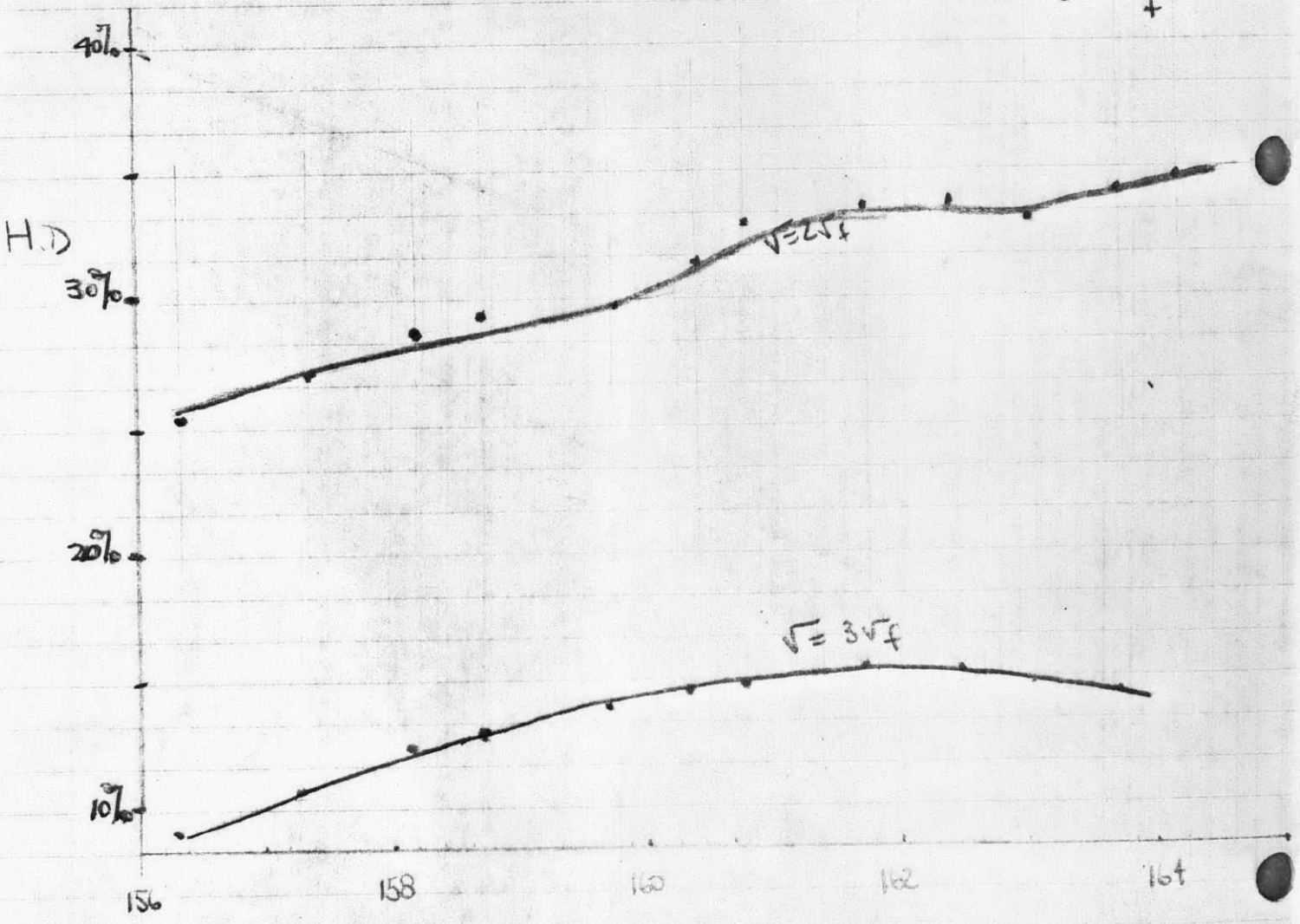

FOOTNOTES

1. Galaitsis, A., Visualization of the Time Average Pressure Distribution in a Rectangular Resonant Cavity, Ph. D. Thesis, Physics, M.I.T., 1972

2. Ross, J.A. Jr.,Non-Linear Interaction between Sound Field and Fluid Surface, M.S. Thesis, Physics, M.I.T., 1969

3. Andrade, E., On Solid Particles Under the Influence of Air Vibrations in Tubes, Philosophical Transactions of the Royal Society, A230, London, 1932

4. Andrade, op. cit.

5. Rayleigh, J., On the Cirulation of Air Observed in Kundt's Tube and Some Allied Acoustical Problems, Philosophical Transactions of the Royal Society, A175, London, 1883

6. Bruel and Kjaer Microphone Instruction Manual, Denmark, 1963

REFERENCES

1. Andrade, E., On Solid Particles Under the Influence of Air Vibrations in Tubes, Philosophical Transactions of the Royal Society, A230, London, 1932

2. Bruel and Kjaer Microphone Instruction Manual, Denmark, 1963

3. Galaitsis, A., Doctoral Thesis, Physics, M.I.T., 1972

4. Morse, P., Thermal Physics, W.A. Benjamin, New York, 1969

5. Morse, P. and Ingard, K.U., Theoretical Acoustics, McGraw-Hill New York, 1968

6. Rayleigh, J., On the Circulation of Air in Kundt's Tubes and Some Allied Acoustical Problems, Philosophical Transactions of the Royal Society, A175, London, 1883

7. Ross, J.A. Jr., M.S. Thesis, Physics, M.I.T., 1969

ACKNOWLEDGEMENTS

I wish to thank Prof. Ingard and Tony Galaitsis for their help and advice.

I also wish to thank the Research Laboratory of Electronics, the Acoustics Laboratory of the Mechanical Engineering Dept., the Gas Turbine Lab, and the Chemistry Department for the use of their excellent facilities.